



RESEARCH PAPER

Rice transcription factor OsMYB102 delays leaf senescence by down-regulating abscisic acid accumulation and signaling

Weilan Piao^{1,*}, Suk-Hwan Kim^{1,*}, Byoung-Doo Lee¹, Gynheung An², Yasuhito Sakuraba^{1,†,‡} and Nam-Chon Paek^{1,‡}

¹ Department of Plant Science, Plant Genomics and Breeding Institute, Research Institute of Agriculture and Life Sciences, Seoul National University, Seoul 08826, Republic of Korea

² Department of Plant Molecular Systems Biotechnology, Crop Biotech Institute, Kyung Hee University, Yongin 17104, Republic of Korea

[†] Present address: Graduate School of Agricultural and Life Sciences, Biotechnology Research Center, The University of Tokyo, Tokyo 113–8657, Japan.

* These authors have contributed equally to this work.

[‡] Correspondence: usakurab@mail.ecc.u-tokyo.ac.jp or n CPAEK@snu.ac.kr

Received 29 June 2018; Editorial decision 18 February 2019; Accepted 18 February 2019

Editor: Dabing Zhang, Shanghai Jiao Tong University, China

Abstract

MYB-type transcription factors (TFs) play important roles in plant growth and development, and in the responses to several abiotic stresses. In rice (*Oryza sativa*), the roles of MYB-related TFs in leaf senescence are not well documented. Here, we examined rice MYB TF gene *OsMYB102* and found that an *OsMYB102* T-DNA activation-tagged line (termed *osmyb102-D*), which constitutively expresses *OsMYB102* under the control of four tandem repeats of the 35S promoter, and *OsMYB102*-overexpressing transgenic lines (*35S:OsMYB102* and *35S:GFP-OsMYB102*) maintain green leaves much longer than the wild-type under natural, dark-induced, and abscisic acid (ABA)-induced senescence conditions. Moreover, an *osmyb102* knockout mutant showed an accelerated senescence phenotype under dark-induced and ABA-induced leaf senescence conditions. Microarray analysis showed that a variety of senescence-associated genes (SAGs) were down-regulated in the *osmyb102-D* line. Further studies demonstrated that overexpression of *OsMYB102* controls the expression of SAGs, including genes associated with ABA degradation and ABA signaling (*OsABF4*, *OsNAP*, and *OsCYP707A6*), under dark-induced senescence conditions. *OsMYB102* inhibits ABA accumulation by directly activating the transcription of *OsCYP707A6*, which encodes the ABA catabolic enzyme ABSCISIC ACID 8'-HYDROXYLASE. *OsMYB102* also indirectly represses ABA-responsive genes, such as *OsABF4* and *OsNAP*. Collectively, these results demonstrate that *OsMYB102* plays a critical role in leaf senescence by down-regulating ABA accumulation and ABA signaling responses.

Keywords: Abscisic acid, chlorophyll degradation, leaf senescence, *OsCYP707A6*, *OsMYB102*, rice, senescence-associated genes, transcriptional regulation.

Introduction

Leaf senescence is the final stage of leaf development, in which intracellular organelles and macromolecules are actively destabi-

lized to relocate nutrients into developing tissues or storage organs (Lim *et al.*, 2007). The initiation of leaf senescence is tightly regulated by endogenous factors, such as phytohormones and metabolites (Moore *et al.*, 2003; Sakuraba *et al.*,

2012; Kusaba *et al.*, 2013), and external stimuli, such as light, drought, high salinity, and pathogens (Bohnert *et al.*, 1995; Quirino *et al.*, 1999; Sakuraba *et al.*, 2014, 2018).

One of the best approaches for understanding the mechanisms behind leaf senescence is the isolation and analysis of stay-green (also termed non-yellowing) mutants, which show a delayed leaf senescence phenotype. To date, a large number of stay-green mutants have been identified in model and crop plant species. The characterization of several of these stay-green mutants and examination of transcriptional changes during leaf senescence in wild-type (WT) plants have helped in the identification of many senescence-associated genes (SAGs; Hörtensteiner, 2009; Kusaba *et al.*, 2013).

Transcription factors (TFs) play essential roles in the regulation of gene expression (Ptashne and Gann, 1990). To date, a number of TFs have been shown to regulate leaf senescence in the model dicot Arabidopsis and in a few crop plants. The plant-specific NAC (NAM/ATAF/CUC) TFs are one of the largest families of plant TFs (Ooka *et al.*, 2003). In Arabidopsis, several NAC TFs (ANAC002/ATAF1, ANA016, ANAC019, ANAC029/NAP, ANAC046, ANAC055, ANAC072/RD26, and ANAC092/ORE1) act as positive regulators of leaf senescence; their null mutants show a stay-green phenotype during senescence (Kim *et al.*, 2009; Kim *et al.*, 2013; Takasaki *et al.*, 2015; Oda-Yamamizo *et al.*, 2016). By contrast, ANAC042/JUB1 and ANAC083/VNI2 have been identified as negative regulators of leaf senescence (Yang *et al.*, 2011; Wu *et al.*, 2012).

Senescence-associated NAC (senNAC) TFs have also been identified in crop plants. In rice (*Oryza sativa*), RNA interference-mediated gene silencing lines of *OsNAC2* and *OsNAP*, and *OsNAC106*-overexpressing (*OsNAC106*-OX) plants showed a stay-green phenotype under natural and dark-induced senescence conditions (Liang *et al.*, 2014; Sakuraba *et al.*, 2015; Mao *et al.*, 2017). Remarkably, these stay-green rice plants showed an increase in crop yield, indicating that the stay-green trait may prove useful to enhance crop yield.

In addition to NAC TFs, other TF families, including WRKY and basic helix-loop-helix (bHLH) TFs, have important roles in the regulation of leaf senescence (Miao *et al.*, 2004; Besseau *et al.*, 2012). A few bHLH TFs have a critical role in promoting leaf senescence in Arabidopsis and rice; for example, PHYTOCHROME INTERACTING FACTOR (PIF) TFs function in dark-induced leaf senescence (Sakuraba *et al.*, 2014, 2017) and MYC TFs act in methyl jasmonate (MeJA)-induced leaf senescence (Qi *et al.*, 2015; Uji *et al.*, 2017).

MYB (myeloblastosis) TFs are present in all eukaryotes and comprise one of the largest TF groups in plants; there are at least 197 and 155 MYB genes in Arabidopsis and rice, respectively (Katiyar *et al.*, 2012). Plant MYB TFs are mainly classified into three groups with varying numbers of MYB domain repeats that determine their ability to bind DNA: the MYB-related group (one MYB domain), the R2R3-type group (two MYB domains), and the R1R2R3-MYB group (three MYB domains) (Chen *et al.*, 2006; Du *et al.*, 2009). The largest group is the R2R3-MYBs, and 138 of the 197 Arabidopsis MYBs are classified as R2R3-MYBs (Katiyar *et al.*, 2012). Plant MYB TFs play important roles in various biological processes, including secondary metabolism, cell cycle regulation, phytohormone

signal transduction, disease resistance, and abiotic stress tolerance (Cominelli and Tonelli, 2009; Baldoni *et al.*, 2015; Liu *et al.*, 2015).

A few transcriptome analyses indicated the importance of MYB TFs in the onset of leaf senescence (Balazadeh *et al.*, 2008; Moschen *et al.*, 2016). MYBH acts as a positive regulator of leaf senescence, since the *mybh* mutants show a stay-green phenotype and the *MYBH*-OX lines exhibit an early leaf yellowing phenotype under both natural and dark-induced leaf senescence conditions (Huang *et al.*, 2015). In addition, SMALL AUXIN UPREGULATED 36 (SAUR36), a key regulator of auxin-induced leaf senescence (Hou *et al.*, 2013), is strongly up-regulated in the *MYBH*-OX lines (Huang *et al.*, 2015), indicating the importance of MYBH in the regulation of auxin-induced leaf senescence. By contrast, Arabidopsis MYB44 (AtMYB44), an R2R3-type MYB TF, is a negative regulator of leaf senescence; *AtMYB44*-OX lines have delayed leaf senescence and *atmyb44* knockout mutants have accelerated leaf yellowing during senescence (Jaradat *et al.*, 2013). In addition, AtMYB44 directly activates or regulates a few SAGs, including *WRKY70* and *ETHYLENE INSENSITIVE2 (EIN2)* (Liu *et al.*, 2011; Besseau *et al.*, 2012). Considering that several MYB TFs have been shown to regulate leaf senescence in Arabidopsis, other plant species, such as rice, will likely have senescence-associated MYB (senMYB) TFs.

In this study, we identified and characterized a rice senMYBTF, OsMYB102 (Os06g43090). We used a T-DNA-mediated activation-tagged line of *OsMYB102*, termed *osmyb102-D*, which constitutively expressed *OsMYB102* under the control of four tandem repeats of the 35S promoter and generated *OsMYB102*-overexpressing transgenic lines (35S:*OsMYB102* and 35S:*GFP*-*OsMYB102*), all of which showed a strong stay-green phenotype during both natural and dark-induced senescence. By contrast, leaf discs of an *osmyb102* knockout mutant generated by CRISPR/Cas9 showed an early leaf yellowing phenotype during leaf senescence. Microarray analysis revealed that in addition to a number of SAGs, genes associated with abscisic acid (ABA) metabolism and responses were differentially expressed in the *osmyb102-D* line during dark-induced leaf senescence compared with the WT. We revealed that the OsMYB102 TF directly activates the expression of *CYTOCHROME P450*, *FAMILY 707*, *SUBFAMILY A*, *POLYPEPTIDE 6* (OsCYP707A6), which encodes an ABA catabolic enzyme, and indirectly represses the expression of *NAC-LIKE ACTIVATED BY AP3/PI* (OsNAP) and *ABA-RESPONSIVE ELEMENT BINDING FACTOR 4* (OsABF4), which encode TFs associated with the ABA signal response. Furthermore, OsABF4 directly activates the expression of *STAYGREEN* (OsSGR) and *NON-YELLOW COLORING 1* (OsNYC1), which encode chlorophyll (Chl) catabolic enzymes. Therefore, OsMYB102 may regulate leaf senescence by inhibiting ABA accumulation and signaling, as well as Chl catabolism.

Materials and methods

Plant materials and growth conditions

The *osmyb102-D* mutant and its parental WT japonica rice cultivar 'Dongjin' were grown in a growth chamber under long-day [LD; 14.5 h

light (300 $\mu\text{mol m}^{-2} \text{s}^{-1}$), 30 °C/9.5 h dark, 24 °C] conditions or in a paddy field under natural LD (>14 h light/day) conditions in Suwon, Korea (37°N latitude). The seeds were sown on seedbeds in a greenhouse and after 1 month the seedlings were transplanted to the paddy field. The T-DNA insertion line *osmyb102-D* (stock number: PFG_3A-01050) was obtained from the Crop Biotech Institute at Kyung Hee University, Korea. Rice plants were also grown in growth chambers under LD (14.5 h light, 30 °C/9.5 h dark, 24 °C) conditions using light-emitting diodes at a photon flux density of approximately 300 $\mu\text{mol m}^{-2} \text{s}^{-1}$ of photosynthetically active radiation, with 60% relative humidity. For dark-induced senescence (DIS), detached or attached leaves of 3-week-old plants were incubated in complete darkness.

Plasmid construction and transformation

The *OsMYB102* cDNA was amplified by RT-PCR using gene-specific primers (see [Supplementary Table S1](#) at *JXB* online) and sub-cloned into pCR8/GW/TOPO ligated into the pMDC32 and pMDC43 gateway binary vectors containing the 35S promoter (Curtis and Grossniklaus, 2003). The 35S:*OsMYB102* construct in the pMDC32 plasmid and the 35S:*GFP-OsMYB102* construct in the pMDC43 plasmid were introduced into calli generated from mature embryos of Dongjin seeds by *Agrobacterium* (strain LBA4404)-mediated transformation (Lee *et al.*, 2006). The transgenic rice plants were selected on 2N6 medium containing hygromycin (50 mg L⁻¹) and confirmed by genomic PCR using specific primers ([Supplementary Table S1](#)).

To generate the *osmyb102* knockout mutant using CRISPR/Cas9, one target sequence in the *OsMYB102* coding region, GAGTTGAGGCGGATTGCGAC, was selected using the CRISPR direct program (<https://crispr.dbcls.jp/>) (Naito *et al.*, 2015). The target sequence, GAGTTGAGGCGGATTGCGAC, was introduced into a single guide RNA (sgRNA) expression cassette in the pOs-sgRNA vector, and the cassette was transferred to the destination vector pH-Ubica9-7 (Miao *et al.*, 2013) by LR reaction using Gateway LR Clonase II Enzyme Mix (Invitrogen). The resulting vector construct was introduced into calli generated from the mature embryos of Dongjin rice seeds by *Agrobacterium*-mediated transformation (Lee *et al.*, 2006). Transgenic rice seedlings were selected by hygromycin resistance and confirmed by direct sequencing of genomic PCR products amplified using target region-specific primers ([Supplementary Table S1](#)).

Chl quantification

To measure total Chl concentrations, pigments were extracted from leaf tissues with 80% ice-cold acetone. Chl concentrations were determined by spectrophotometry as described previously (Porra *et al.*, 1989).

Measurement of ion leakage

Ion leakage was measured as described previously (Lee *et al.*, 2015). Briefly, membrane leakage was determined by measuring electrolytes (or ions) leaking from rice leaf discs (1 cm²). Three leaf discs from each treatment were immersed in 6 ml of 0.4 M mannitol at room temperature with gentle shaking for 3 h, and the initial conductivity of the solution was measured with a conductivity meter (CON 6 Meter, LaMotte Co., USA). Total conductivity was determined after incubation of the samples at 85 °C for 20 min. The ion leakage rate is expressed as a percentage (initial conductivity divided by total conductivity).

SDS-PAGE and immunoblot analysis

Total protein extracts were prepared from leaf tissues using the middle section of the third leaf in the main culm of 2-month-old rice plants grown in the growth chamber under LD conditions. Leaf tissues were ground in liquid nitrogen, and 10-mg aliquots were homogenized with 100 μl of sample buffer (50 mM Tris pH 6.8, 2 mM EDTA, 10% glycerol, 2% SDS, and 6% β -mercaptoethanol). The homogenates were centrifuged at 10 000 *g* for 3 min, and the supernatants were denatured at 80 °C for 5 min. A 4- μl aliquot of each sample was subjected to 12% (w/v) SDS-PAGE, followed by

electroblotting onto a Hybond-P membrane (GE Healthcare). Antibodies against photosystem proteins, including Lhca1, Lhca2, Lhcb1, Lhcb2, and CP43, were used for immunoblot analysis, and RbcL was visualized by Coomassie Brilliant Blue (CBB) staining. The level of each protein was examined using the ECL system with WESTSAVE (AbFRONTIER, Korea) according to the manufacturer's protocol.

Measurement of F_v/F_m ratios

The F_v/F_m ratios of flag leaf tissues of WT and *osmyb102-D* plants grown in the paddy field were measured using an OS-30p instrument (Opti Sciences, USA), as previously described (Sakuraba *et al.*, 2016). The middle section of each flag leaf was adapted in the dark for 5 min for complete oxidation of QA. After the dark treatment, the F_v/F_m ratio was measured in the paddy field. For both experiments, we conducted more than three experimental replicates per plant.

RNA isolation and reverse transcription-quantitative PCR analysis

For the reverse transcription reactions, total RNA was extracted from rice leaf blades and other tissues using an RNA Extraction Kit (Macrogen, Seoul, Korea). First-strand cDNA was prepared with 2 μg total RNA using M-MLV reverse transcriptase and oligo(dT)₁₅ primers (Promega) in a total volume of 25 μl and diluted with 75 μl water. For quantitative PCR (qPCR), a 20 μl mixture was prepared including first-strand cDNA equivalent to 2 μl total RNA, 10 μl 2 \times GoTaq master mix (Promega), 6 μl distilled water, and gene-specific forward and reverse primers ([Supplementary Table S1](#)). The qPCR was performed using a LightCycler 480 (Roche Diagnostics). Rice *Ubiquitin5* (*UBQ5*) was used as an internal control. The relative expression level of each gene was calculated using the 2^{- $\Delta\Delta\text{CT}$} method as previously described (Livak and Schmittgen, 2001).

Microarray analysis

The 1-month-old WT (Dongjin) and *osmyb102-D* plants grown under LD conditions were incubated in darkness for 3 d. Total RNA was extracted from the second leaves using TRIzol Reagent (Invitrogen) according to the manufacturer's protocol. RNA quality was checked using a 2100 Bioanalyzer (Agilent Technologies). Microarray analysis was performed using the Rice Gene Expression Microarray, design identifier 015241 (Agilent), containing 43 803 rice genes. Total RNA (150 ng) was used to prepare the Cy3-labeled probes using the Low RNA Input Linear Amplification Kit PLUS (Agilent). Labeled RNA probes were fragmented using the Gene Expression Hybridization buffer kit (Agilent). The arrays were air-dried and scanned using a high-resolution array scanner (Agilent) with the appropriate settings for two-color gene expression arrays. GeneSpring GX 7.3 (Agilent) was used to calculate the intensity ratio and fold changes. Microarray analysis was performed in two experimental replicates with two different biological replicates of WT and *osmyb102-D* plants. For evaluating the statistical significance and obtaining the *P*-value, one-sample *t*-tests were performed using GeneSpring GX 7.3 (Agilent). Differentially expressed genes (DEGs) were selected for *P*<0.05 and normalized *osmyb102-D*/WT ratios >2 or <0.5. These DEGs were used for the Venn diagram. The information on phytohormone-associated genes was obtained from Oryzabase (www.shigen.nig.ac.jp/rice/oryzabase).

Yeast one-hybrid assays

For the yeast one-hybrid assays, the *OsMYB102* coding sequence was inserted into the pGAD424 vector (Clontech) as prey. DNA fragments corresponding to the promoters (750 bp) of *OsCYP707A6* were cloned into pLacZi (Clontech) as bait. For each gene, two DNA fragments (-1500 to -751 and -750 to -1 from the start codon) were prepared. Primers used for cloning are listed in [Supplementary Table S1](#). The yeast strain YM4271 was used for bait and prey clones, and β -galactosidase activity was measured by liquid assay using chlorophenol

red- β -D-galactopyranoside (CPRG; Roche Applied Science) according to the *Yeast Protocol Handbook* (Clontech).

Chromatin immunoprecipitation assays

For the chromatin immunoprecipitation (ChIP) assay, the 35S:*OsMYB102-MYC* and 35S:*OsABF4-MYC* constructs in the pEarly Gate 203 binary vector (Earley *et al.*, 2006) were transfected into rice protoplasts as previously described (Zhang *et al.*, 2011). The protoplasts were then subjected to crosslinking for 20 min with 1% formaldehyde under vacuum. The chromatin complexes were isolated and sonicated as previously described (Saleh *et al.*, 2008). An anti-Myc polyclonal antibody (Abcam) and Protein A agarose/salmon sperm DNA (Millipore) were used for immunoprecipitation. After reversing the crosslinking and protein digestion, the DNA was purified using a QIAquick PCR Purification kit (Qiagen). The primer sequences for each gene are listed in Supplementary Table S1.

Protoplast transient assays

To construct reporter plasmids containing the luciferase (*LUC*) reporter gene under the control of various promoters, promoter fragments of *OsCYP707A6* (−1516 to −1), *OsNAP* (−1502 to −1), *OsABF4* (−1516 to −1), *OsSGR* (−1514 to −1), and *OsNYC1* (−1508 to −1) were cloned into the pGreenII-0579 vector, which contains the *LUC* reporter gene at the C-terminus. For the effector plasmids, the cDNAs of *OsMYB102*, *OsNAP*, and *OsABF4* were cloned into the pCR8/GW/TOPO Gateway vector (Invitrogen). Then, these cDNAs were recombined into the pEarley203 vector (Earley *et al.*, 2006). The reporter (4 μ g) and effector plasmids (8 μ g) were co-transfected into 5×10^4 rice protoplasts by the polyethylene glycol-mediated transfection method (Yoo *et al.*, 2007). Transfected protoplasts were then suspended in protoplast culture medium (0.4 mM mannitol, 4 mM MES buffer, and 15 mM MgCl₂, pH 5.8) and maintained in darkness for 16 h. The *LUC* activity in each cell lysate was determined using the Luciferase Assay System Kit (Promega).

Quantification of ABA contents

To determine the level of ABA accumulation, leaf discs from 1-month-old plants were collected and weighed. The leaves were ground in liquid nitrogen and homogenized with 80% methanol containing 1 mM butylated hydroxytoluene overnight at 4 °C to extract ABA. The ABA content was analysed using an ABA ELISA Kit (MyBiosource, San Diego, CA, USA).

Results

OsMYB102 delays natural senescence

In naturally senescing leaf blades in rice, *OsMYB102* was highly expressed in the yellowing sector (Fig. 1A; region c) compared with the green sectors (Fig. 1A; regions a and b), and its expression decreased in the fully senesced yellow sector (Fig. 1A; region d). Similarly, *OsMYB102* expression increased substantially until 3 d of dark incubation (DDI) (Fig. 1B), suggesting that *OsMYB102* encodes a senMYB.

To elucidate the physiological function of *OsMYB102* in leaf senescence, we searched for rice mutant lines in the Rice GE database (<http://signal.salk.edu/cgi-bin/RiceGE>) and found an activation-tagged line, PFG_3A-01050, in which a single T-DNA fragment containing four tandem repeats (4x) of the 35S promoter is inserted in the promoter of *OsMYB102* (Fig. 1C). Reverse transcription-quantitative PCR (RT-qPCR) analysis confirmed that the leaves of the PFG_3A-01050 line

accumulated much higher levels of *OsMYB102* mRNA compared with its parental *japonica* cultivar ‘Dongjin’ (hereafter termed WT, Fig. 1D). This indicated that the PFG_3A-01050 lines constitutively express *OsMYB102* mRNA under the control of the 35S promoters. Hereafter, we termed this activation-tagged line *osmyb102-D*.

We next examined the phenotype of the *osmyb102-D* line during natural senescence. The plants were grown in the paddy field under natural LD conditions (≥ 14 h light per day at 37°N latitude, Suwon, Korea). At the vegetative stage, there was no significant difference in leaf color between the WT and *osmyb102-D* plants, although the heading date was slightly different (Fig. 1E, left panel). However, during grain filling, the *osmyb102-D* line exhibited a delayed senescence phenotype (Fig. 1E, right panel). The difference in leaf color between the WT and *osmyb102-D* plants was clear in the second leaves (Fig. 1F). Consistent with the delayed senescence phenotype, the leaves of *osmyb102-D* plants retained total Chl levels, which decreased normally in the leaves of WT during natural senescence (Fig. 1G).

To examine the efficiency of the photosynthetic apparatus, we measured the F_v/F_m ratio (a measure of the efficiency of photosystem II; PSII) after heading. The F_v/F_m ratio in the WT decreased drastically after 30 d after heading (DAH) but remained high in the *osmyb102-D* line even at 50 DAH (Fig. 1H). These results indicate that *OsMYB102* functions as a strong negative regulator of leaf senescence and the *osmyb102-D* plants are stay-green mutants.

OsMYB102 delays DIS

To study the delayed senescence caused by overexpression of *OsMYB102* in more detail, we examined the *osmyb102-D* phenotype during DIS using detached leaf discs. Leaf discs from 1-month-old plants were floated on MES buffer (pH 5.8) and incubated in the dark. After 4 DDI, the leaf discs of *osmyb102-D* plants showed a stay-green phenotype while those of the WT turned completely yellow (Fig. 2A). Consistent with the phenotype, the total Chl level remained high in *osmyb102-D* plants during DIS (Fig. 2B). Similarly, all photosystem proteins examined, including PSII antenna proteins (Lhcb1, Lhcb2, and Lhca1) and core proteins (CP43), and PSI antenna proteins (Lhca2), remained stable in *osmyb102-D* plants at 3 and 4 DDI, while all photosystem proteins decreased to undetectable levels in the WT (Fig. 2C). Additionally, the ion leakage rate, an indicator of membrane integrity, was also significantly lower in *osmyb102-D* plants than in the WT (Fig. 2D).

To verify that the overexpression of *OsMYB102* causes the delay of leaf senescence, we generated rice transgenic lines overexpressing the full-length cDNA of *OsMYB102* (hereafter termed 35S:*OsMYB102*) as well as *OsMYB102* fused with a gene encoding green fluorescent protein (GFP) at the N-terminus (hereafter termed 35S:*GFP-OsMYB102*). By RT-qPCR, we found that *OsMYB102* was significantly up-regulated in both 35S:*OsMYB102* and 35S:*GFP-OsMYB102* transgenic lines (Fig. 3A). During DIS, these lines exhibited a strong stay-green phenotype, similar to the *osmyb102-D* line (Fig. 3B), and retained total Chl levels (Fig. 3C).

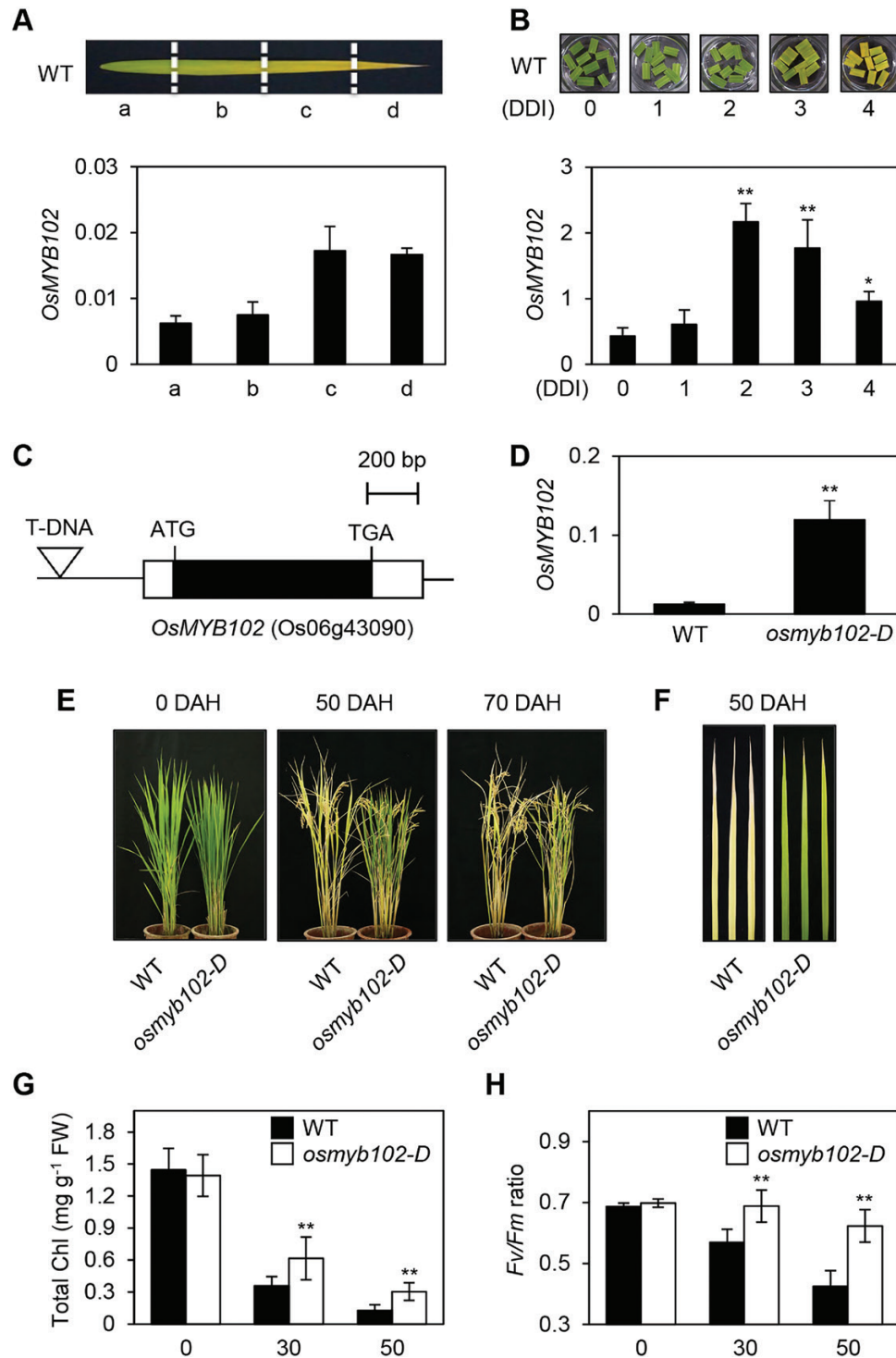


Fig. 1. *osmyb102-D* plants showed a delayed-senescence phenotype in natural paddy field conditions. (A, B) The relative transcript levels of *OsMYB102* in senescing WT leaves (A) or detached leaf discs during DIS (B) were determined by RT-qPCR and normalized to the transcript levels of *UBQ5*. The mean and SD values were obtained from more than three biological samples. DDI, day(s) of dark incubation. (C) Gene structure of *OsMYB102* and the T-DNA insertion site. (D) The relative transcript level of *OsMYB102* in *osmyb102-D* was determined by RT-qPCR and normalized to the transcript level of *UBQ5*. (E, F) Phenotypes of the WT (the parental *japonica* rice cultivar 'Dongjin') and the *osmyb102-D* plants at 0, 50, and 70 DAH. (G, H) Changes of total Chl levels (G) and *F_v/F_m* ratios (H) in the WT and *osmyb102-D* plants during grain filling (0–50 DAH). The mean and SD values were obtained from more than five biological samples. These experiments were repeated twice with similar results. DAH, days after heading. Asterisks indicate significant difference compared with the expression level of *OsMYB102* at 0 DDI (B), or difference between the WT and *osmyb102-D* (D, G, H) (Student's *t*-test, **P*<0.05, ***P*<0.01).

We further generated an *osmyb102* knockout mutant using CRISPR/Cas9. The *osmyb102* mutant has a one-base insertion in the exon of *OsMYB102*, resulting in a premature stop

codon (Supplementary Fig. S1A, B). In contrast with the phenotype of *osmyb102-D* and *OsMYB102* overexpressors, the leaf discs of *osmyb102* knockout mutant showed an early leaf

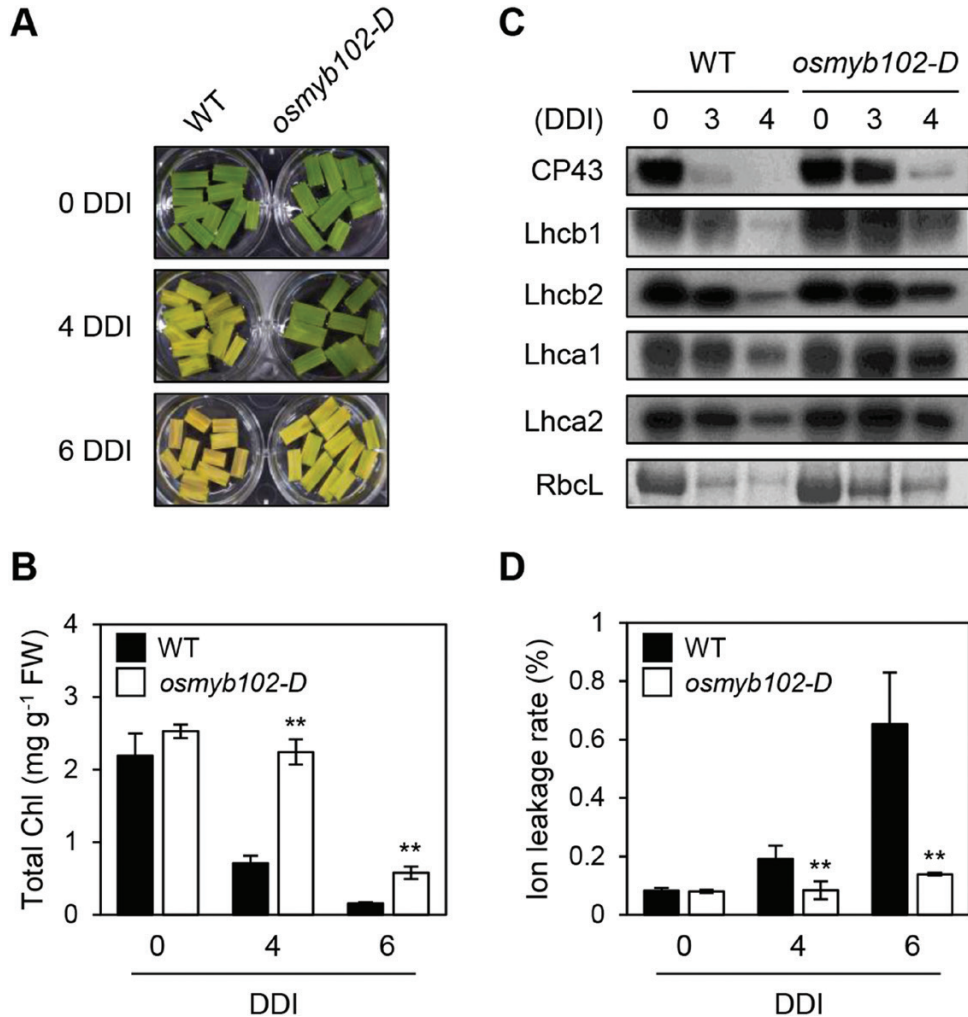


Fig. 2. *osmyb102-D* plants showed a delayed senescence phenotype during dark-induced senescence. (A–D) Changes of detached leaf color (A), total Chl levels (B), photosystem protein levels (C), and ion leakage rates (D) in the leaf discs of the WT and *osmyb102-D* plants during dark incubation. Leaf segments were incubated on 3 mM MES (pH 5.8) buffer with the abaxial side up at 28 °C in darkness and sampled at the specified DDI for each experiment. (C) Antibodies against PSII antenna (Lhcb1 and Lhcb2), PSI antenna (Lhca1 and Lhca2), and PSII core (CP43) proteins were used for immunoblot analysis. RbcL was detected by Coomassie Brilliant Blue staining. (B, D) Black and white bars indicate the WT and *osmyb102-D* plants, respectively. The mean and SD values were obtained from more than five leaf samples. Asterisks indicate a significant difference between the WT and *osmyb102-D* plants (Student's *t*-test, **P*<0.05, ***P*<0.01). These experiments were repeated three times with similar results. DDI, day(s) of dark incubation.

yellowing phenotype at 4 DDI (Supplementary Fig. S1C, D). Collectively, these results indicate that the overexpression of *OsMYB102* delays leaf senescence by maintaining the integrity of photosystem complexes and cell membranes.

The transcript levels of SAGs and ABA-related genes are altered in *osmyb102-D* plants during DIS

To examine the regulatory network behind *OsMYB102*-mediated leaf senescence, we conducted a genome-wide microarray analysis to identify DEGs between *osmyb102-D* and WT plants. One-month-old whole plants were incubated in the dark for 4 d (4 DDI), and their leaves were sampled prior to and after dark induction for microarray analysis (Fig. 4A). We identified 1026 and 2785 genes that were up-regulated (*osmyb102-D*/WT; >2) and 915 and 3890 genes that were down-regulated (*osmyb102-D*/WT; <0.5) at 0 and 4 DDI, respectively (Fig. 4B, C).

Among the phytohormones, ABA, ethylene, jasmonic acid (JA), salicylic acid (SA), strigolactone, gibberellic acid, and brassinosteroids promote senescence, and cytokinin and auxin inhibit senescence (Kusaba et al., 2013). Therefore, we first investigated whether phytohormone-associated genes are differentially expressed in *osmyb102-D* plants compared with the WT (*osmyb102-D*/WT). The expression of the phytohormone signaling and biosynthesis genes (Supplementary Fig. S2), especially those involved in the ABA pathways, were significantly down-regulated in the *osmyb102-D* line at 4 DDI. By contrast, several auxin biosynthesis and signaling genes were significantly up-regulated in the *osmyb102-D* line at 4 DDI, suggesting that *OsMYB102* is involved in the homeostasis or signaling of phytohormones during leaf senescence, which probably contributes to the delayed senescence phenotype of *osmyb102-D* plants during DIS (Fig. 2).

In addition to phytohormone metabolism and signaling genes, a number of SAGs were down-regulated in the *osmyb102-D*

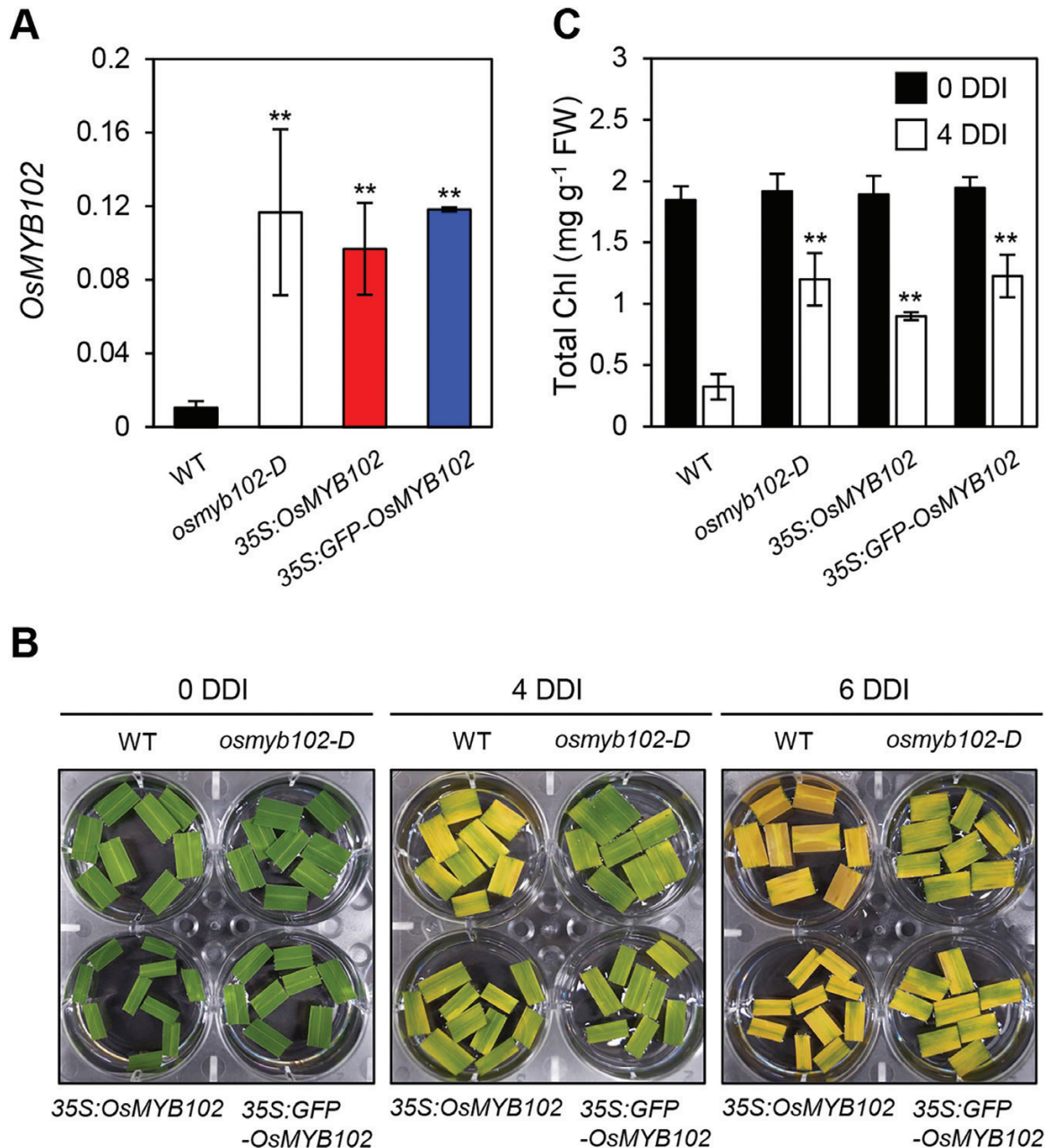


Fig. 3. *OsMYB102*-overexpressing transgenic rice plants show a stay-green phenotype during dark-induced leaf senescence. (A) The expression levels of *OsMYB102* in leaf blades from 1-month-old WT, *osmyb102-D*, 35S:*OsMYB102*, and 35S:GFP-*OsMYB102* plants. The transcript levels of *OsMYB102* were determined by RT-qPCR and were normalized to the transcript levels of *UBQ5*. (B, C) The changes of leaf color (B) and total Chl content (C) in WT, *osmyb102-D*, 35S:*OsMYB102*, and 35S:GFP-*OsMYB102* detached leaf discs during dark-induced leaf senescence. Asterisks indicate a significant difference compared with the WT (Student's *t*-test, ***P*<0.01). The mean and SD values were obtained from more than five leaf samples.

line (Fig. 4D). Among them, *OsCYP707A6*, encoding the ABA catabolic enzyme ABSCISIC ACID 8'-HYDROXYLASE (Yang and Choi, 2006), was up-regulated, while *OsNAP*, encoding a senescence-associated NAC TF (Liang et al., 2014), *STAYGREEN* (*OsSGR*), encoding a Mg-decalatase (Park et al., 2007), and *SALICYLIC ACID 3-HYDROXYLASE* (*OsS3H*), encoding a salicylic acid catabolic enzyme (Zhang et al., 2013), were down-regulated in *osmyb102-D* plants, even in non-senescent leaves (Fig. 4D). Some known SAGs, such as *OsCOI1b* (Lee et al., 2015) and *OsPHYB* (Piao et al., 2015), were not differentially expressed in *osmyb102-D* plants (Fig. 4D), whereas the expression levels of some genes that are

generally down-regulated by senescence (senescence down-regulated genes; SDGs), such as *Lhcb3*, *Lhca1*, *Lhca3*, and *PsaE* (which encode photosystem proteins), remained at high level in *osmyb102-D* plants at 4 DDI (Fig. 4D).

Subsequently, we examined the expression patterns of ABA metabolism and signal responsive genes, SAGs, and SDGs during DIS in *osmyb102-D* and *OsMYB102*-OX (35S:*OsMYB102* and 35S:GFP-*OsMYB102*) plants using RT-qPCR (Fig. 5). Consistent with the microarray results, the expression level of *OsCYP707A6*, which normally decreases in dark-induced and naturally senescing leaves (Supplementary Fig. S3), was strongly up-regulated in the *osmyb102-D* and *OsMYB102*-OX

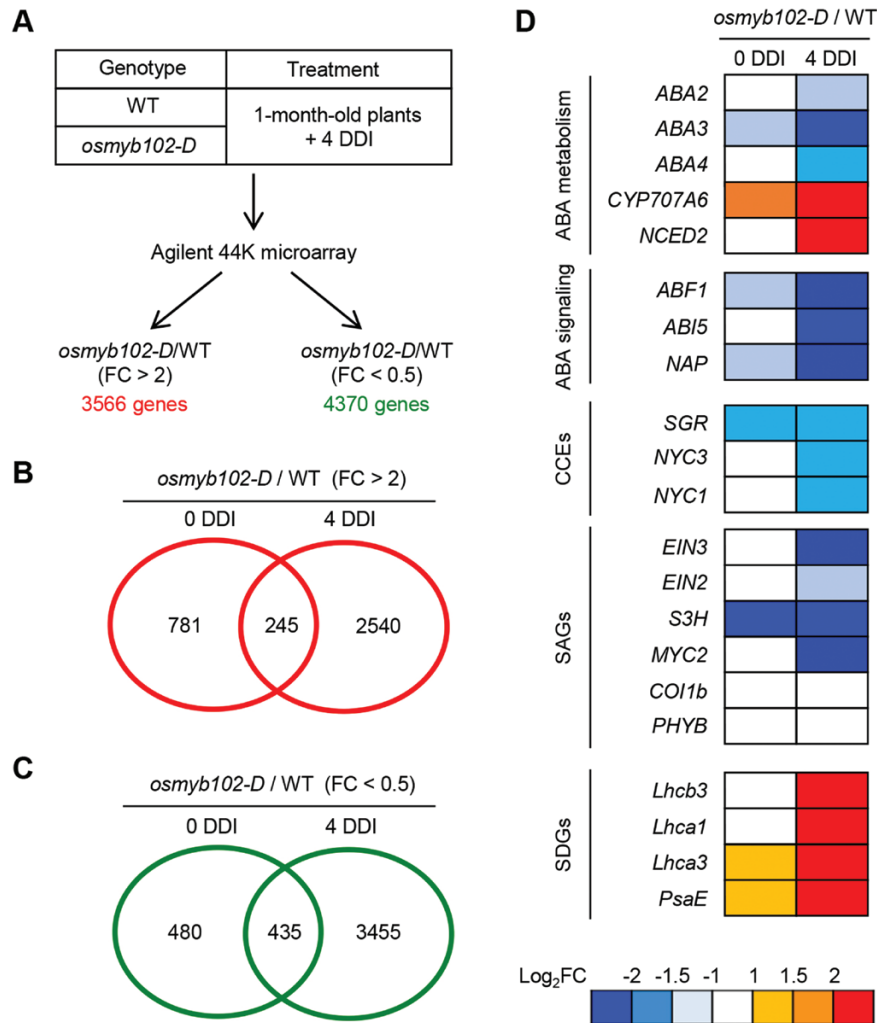


Fig. 4. Altered expression of SAGs in *osmyb102-D* plants during DIS. (A) Summary of the microarray analysis. A filter for Student's *t*-test *P*-value of <0.05 was applied to the differentially expressed genes (DEGs). (B, C) Venn diagrams of the number of DEGs in *osmyb102-D* plants compared with the WT. The numbers of up-regulated (B) and down-regulated (C) genes in *osmyb102-D* plants at 0 and 4 DDI are shown. (D) The ratios of expression levels (*osmyb102-D*/WT) for known or putative SAGs at 0 and 4 DDI. The relative expression value was normalized to the WT expression level. DDI, day(s) of dark incubation.

lines independent of the dark treatment (Fig. 5A). In contrast, the expression levels of ABA-signaling genes (*OsABF1*, *OsABF4*, and *OsNAP*) and other SAGs (*OsSGR*, *OsNYC1*, and *OsEIN3*), which normally increase during DIS, were down-regulated in the *osmyb102-D* and *OsMYB102-OX* lines during DIS (Fig. 5D–I). These results indicate that the expression of *OsMYB102* affects the transcription of a number of SAGs and SDGs.

OsMYB102 directly up-regulates the transcription of *OsCYP707A6*

As shown above, the expression of *OsCYP707A6*, encoding an ABA catabolic enzyme (Yang and Choi, 2006), was significantly up-regulated in the *osmyb102-D* and *OsMYB102-OX* lines even at the vegetative stage (Figs 4D, 5A). Arabidopsis MYB44 (AtMYB44), an R2R3-type MYB TF and the closest homolog of *OsMYB102*, binds to the AACXG sequences on the promoters of target genes (Jung et al., 2012). To examine the relationship between *OsMYB102* and *OsCYP707A6*, we

examined the promoter of *OsCYP707A6* (–1500 to –1 from the ATG) and found that it contains four AACXG sequences (Fig. 6A).

First, we used protoplast transient assays to determine the activity of *OsMYB102* in the activation of *OsCYP707A6* transcription. For the reporter construct, the promoter of *OsCYP707A6* (–1516 to –1) was fused with the LUC reporter (Fig. 6B). LUC activity of the *proOsCYP707A6:LUC* plasmid was significantly enhanced when it was co-transfected with the *35S:OsMYB102-MYC* effector plasmid (Fig. 6C). We subsequently examined whether *OsMYB102* directly interacts with the promoter region of *OsCYP707A6* by ChIP using rice protoplasts transiently expressing *OsMYB102-MYC*. *OsMYB102* strongly bound to the region of amplicon-a, which includes three AACXG motifs, but it did not bind to other regions (Fig. 6A, D). Similarly, *OsMYB102* interacted with the promoter of *OsCYP707A6* in a yeast one-hybrid assay (Fig. 6E). The region of amplicon-a contains three AACXG motifs: AACTG (–1208 to –1204 bp), AACTG (–1144 to –1140 bp), and AACAG (–1139 to –1135 bp).

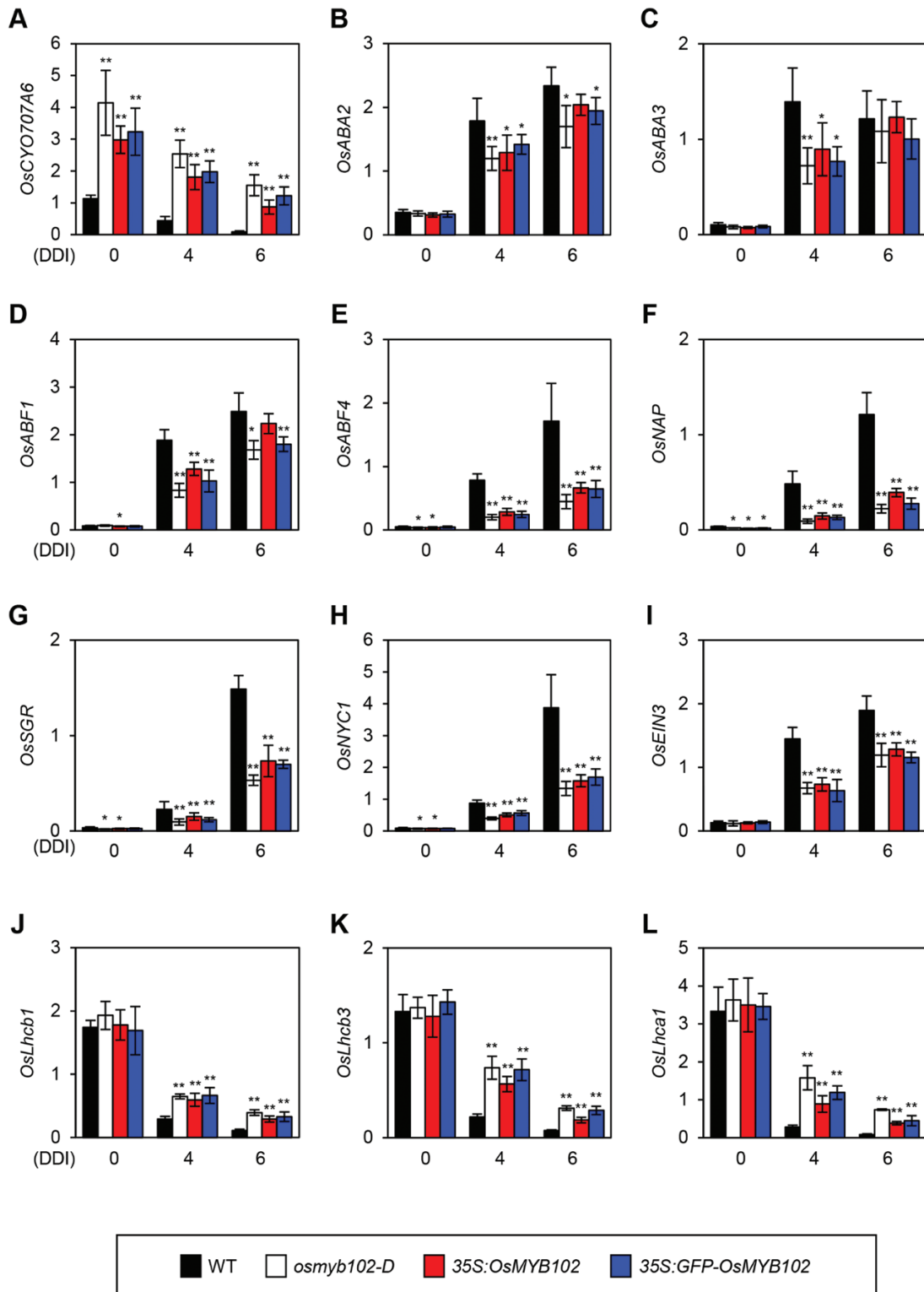


Fig. 5. Altered expression of SAGs and ABA-related genes in WT, *osmyb102-D*, 35S:OsMYB102, and 35S:GFP-OsMYB102 plants under DIS conditions. Plants grown for 1 month under LD (14 h light/day) conditions were transferred to darkness at 28 °C and incubated in darkness for 4 or 6 d. Relative transcript levels of *OsCYP707A6* (A), *OsABA2* (B), *OsABA3* (C), *OsABF1* (D), *OsABF4* (E), *OsNAP* (F), *OsSGR* (G), *OsNYC1* (H), *OsEIN3* (I), *OsLhcb1* (J), *OsLhcb3* (K), and *OsLhca1* (L) were determined by RT-qPCR and normalized to the transcript levels of *UBQ5*. Black, white, red, and blue bars indicate WT, *osmyb102-D*, 35S:OsMYB102, and 35S:GFP-OsMYB102 plants, respectively. The mean and SD values were obtained from more than three biological samples. Asterisks indicate a significant difference compared with the WT (Student's *t*-test, **P*<0.05, ***P*<0.01). These experiments were repeated twice with similar results. DDI, day(s) of dark incubation.

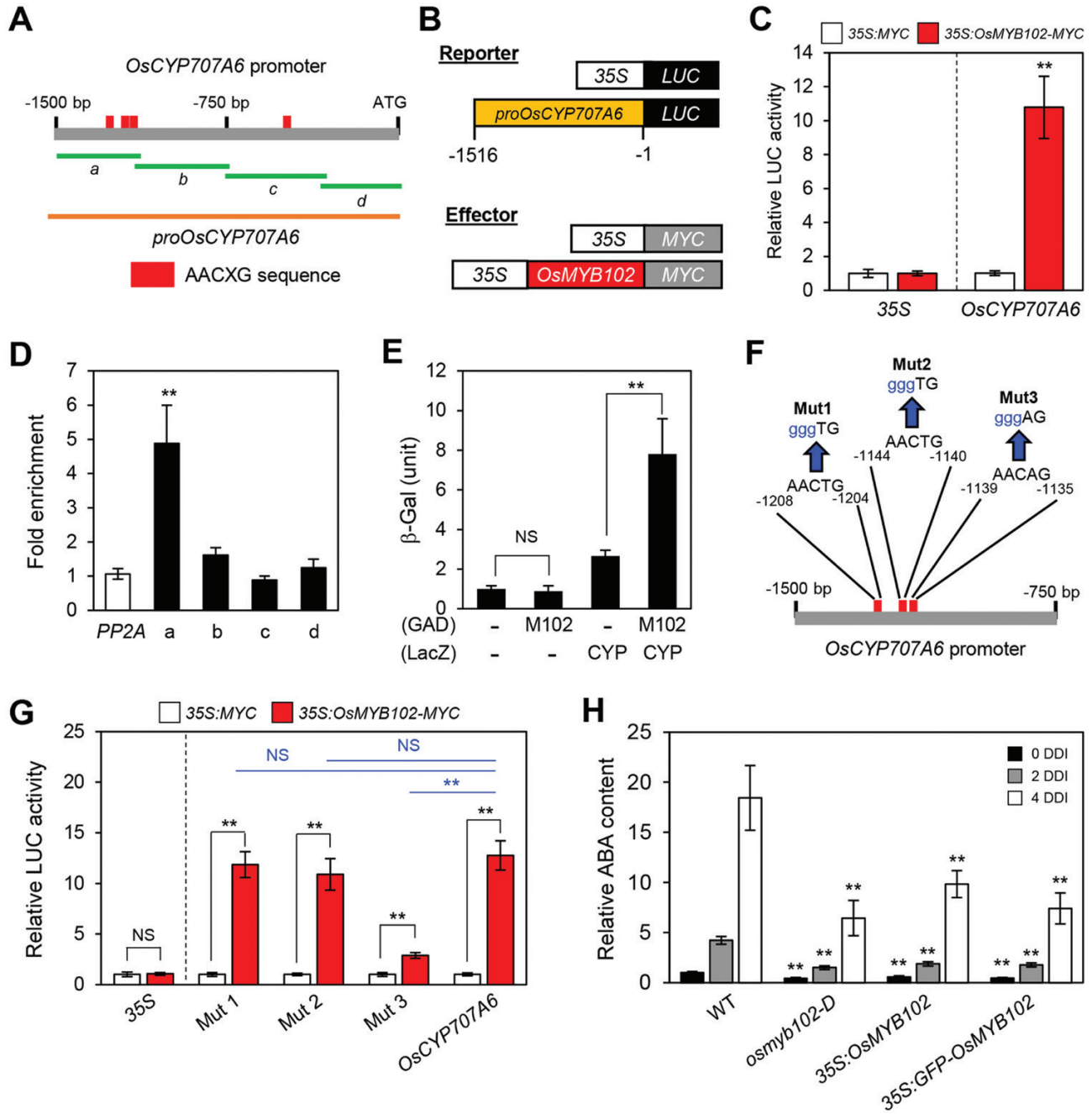


Fig. 6. OsMYB102 directly activates the transcription of *OsCYP707A6*. (A) The positions of the AACXG binding motifs in the promoter of *OsCYP707A6* and promoter fragments used for the ChIP assay (green horizontal lines), the transactivation assay, and Y1H assay (orange horizontal line). (B) Reporter and effector constructs used in the transactivation assay. Each construct also contains the NOS terminator (not shown). (C) The activation of the *OsCYP707A6* promoter (–1516 to –1) by OsMYB102-MYC in the protoplast transient assay. The 35S promoter was used as a negative control. (D) OsMYB102 binding affinity to the promoter region of *OsCYP707A6* *in planta* examined by ChIP assays. OsMYB102-Myc was transiently expressed in protoplasts isolated from 10-day-old WT seedlings. Fold-enrichment of the promoter fragments was measured by immunoprecipitation with an anti-Myc antibody (see Methods). *SERINE/THREONINE PROTEIN PHOSPHATASE 2A* (*PP2A*) was used as a negative control. (E) The binding activity of OsMYB102 to the promoter regions of *OsCYP707A6* was examined by Y1H assays. Empty bait and prey plasmids (–) were used for the negative controls. The relative β -galactosidase activity was obtained by normalizing to the level of each negative control. The mean and SD values were obtained from more than five independent colonies. (F, G) The effects of disruption of the putative OsMYB102 binding sites in the *OsCYP707A6* promoter in rice protoplasts. *LUC* was fused to the wild-type or mutated *OsCYP707A6* promoter fragments, and the *OsMYB102* overexpression vector or empty vector were co-transfected in the protoplasts. The 35S promoter was used as a negative control. The mean and SD values were obtained from more than four biological samples. (H) Relative ABA contents in WT, *osmyb102-D*, 35S:*OsMYB102*, and 35S:*GFP-OsMYB102* plants at 0 (black bars), 2 (gray bars), and 4 d (white bars) after dark incubation. The mean and SD values were obtained from more than five biological samples. (C, D, E, G, H) Asterisks indicate a significant difference compared with the WT or negative control (Student's *t*-test, **P*<0.05, ***P*<0.01).

To determine the binding site of OsMYB102 in the promoter of *OsCYP707A6*, we used protoplast transient assays to examine whether OsMYB102 could activate the promoters of *OsCYP707A6* in which the AACXG sequence was replaced by gggXG (Fig. 6F). The mutated promoter of *OsCYP707A6*, in which the AACAG sequence (−1139 to −1135 bp) was replaced by gggAG, was not strongly activated by co-transfection with OsMYB102, while the substitutions in the two AACTG sequences did not decrease the LUC activity (Fig. 6G), indicating that OsMYB102 directly activates *OsCYP707A6* transcription through binding to the AACAG sequence on the promoter of *OsCYP707A6*.

To examine the effect of activation of *OsCYP707A6* transcription by OsMYB102, we measured ABA contents in WT, *osmyb102-D* plants and two *OsMYB102-OX* lines at 0 and 4 DDI. Regardless of DIS, the ABA levels in the *osmyb102-D* and *OsMYB102-OX* lines were lower compared with the WT (Fig. 6H). Collectively, these results suggest that OsMYB102 is involved in the regulation of ABA accumulation at least in part by directly activating the transcription of *OsCYP707A6*.

OsMYB102 indirectly down-regulates the expression of OsNAP and OsABF4

In addition to *OsCYP707A6*, several ABA signaling genes, such as *OsNAP* and *OsABF4*, were significantly down-regulated in the *osmyb102-D* and *OsMYB102-OX* lines during leaf senescence (Figs 4D, 5E, F). Furthermore, the expression level of *OsMYB102* increased in the WT rice leaves during ABA treatment (Fig. 7A), indicating that OsMYB102 directly or indirectly represses the transcription of *OsNAP* and *OsABF4* in an ABA-dependent manner. To examine the relationship among OsMYB102, *OsNAP*, and *OsABF4*, we searched the promoters of *OsNAP* and *OsABF4* (−1500 to −1 from the ATG) and found that they contained a few AACXG motifs (Fig. 7B).

We then examined the activity of OsMYB102 on the repression of *OsNAP* and *OsABF4* transcription by protoplast transient assays. For the reporter construct, the promoter regions of *OsNAP* (−1502 to −1) and *OsABF4* (−1516 to −1) were fused with the *LUC* reporter gene (Fig. 7C). The LUC activities of the *proOsNAP:LUC* and *proOsABF4:LUC* transgenes were significantly reduced when they were co-transfected with the *35S:OsMYB102-MYC* effector plasmid (Fig. 7D). We used ChIP to examine whether OsMYB102 directly interacts with the promoters of *OsNAP* and *OsABF4* using rice protoplasts transiently expressing OsMYB102-MYC. OsMYB102 did not interact with the promoters of *OsNAP* or *OsABF4* (Fig. 7E), suggesting that OsMYB102 might indirectly represses the transcription of *OsNAP* and *OsABF4*.

Since Arabidopsis NAP and ABF4 homologs have important roles in ABA-induced leaf senescence (Zhao *et al.*, 2016b), it is possible that OsMYB102 is involved in ABA-induced leaf senescence by down-regulating the expression of *OsNAP* and *OsABF4*. To investigate this possibility, we examined the change of leaf color in the *osmyb102-D*, *35S:OsMYB102*, and *35S:GFP-OsMYB102* leaf discs during ABA treatment. After 4 d of a 100 μ M ABA treatment, the *osmyb102-D*,

35S:OsMYB102, and *35S:GFP-OsMYB102* leaf discs showed a stay-green phenotype, retaining high total Chl levels (Fig. 7F, G). By contrast, the leaf discs of the *osmyb102* knockout mutant showed an early leaf yellowing phenotype (Supplementary Fig. S1E, F). These results indicate that OsMYB102 plays an important role in delaying ABA-induced leaf senescence.

OsMYB102 indirectly down-regulates the expression of Chl catabolic enzymes

In this study, we found that *OsSGR* and *OsNYC1*, both of which encode Chl catabolic enzymes (CCEs) (Kusaba *et al.*, 2007; Park *et al.*, 2007), were also down-regulated in the *osmyb102-D* and *OsMYB102-OX* lines (Figs 4D and 5G, H), indicating that OsMYB102 directly or indirectly represses the expression of these CCE genes. OsNAP, functioning downstream of OsMYB102, directly activates transcription of CCE genes, including *OsSGR* and *OsNYC1* (Liang *et al.*, 2014). In addition, Arabidopsis ABF4 also directly activates *AtNYC1* transcription (Gao *et al.*, 2016), although the role of OsABF4 in the regulation of Chl degradation remains unclear. We found that there are several AACXG sequences and an ABRE (ACGTG), which are known binding sequences for ABA bZIP TFs including ABF4 (Choi *et al.*, 2000; Uno *et al.*, 2000), in the promoters of *OsSGR* and *OsNYC1* (Fig. 8A). Therefore, we performed protoplast transient assays to examine the transcriptional relationship among OsMYB102, OsABF4, and these CCEs. For the reporter construct, the promoters of *OsSGR* (−1514 to −1 bp from the start codon) and *OsNYC1* (−1508 to −1 bp from the start codon) were fused with the *LUC* reporter gene (Fig. 8B). The LUC activity from the *proOsSGR:LUC* and *proOsNYC1:LUC* transgenes decreased when they were co-transfected with the *35S:OsMYB102-MYC* effector plasmids (Fig. 8C). By contrast, the LUC activities from the *proOsSGR:LUC* and *proOsNYC1:LUC* transgenes significantly increased when co-transfected with the *35S:OsABF4-MYC* or *35S:OsNAP-MYC* effector plasmids (Fig. 8D).

We subsequently examined whether OsABF4 directly interacts with the promoters of *OsSGR* and *OsNYC1* using a ChIP assay with rice protoplasts transiently expressing OsABF4-MYC. OsABF4 bound to the DNA amplicon-c of the *OsSGR* promoter and to the DNA amplicon-c of the *OsNYC1* promoter, which includes the ABRE binding sequence (Fig. 8E). However, the ChIP assay showed that OsMYB102 did not interact with the promoters of *OsSGR* or *OsNYC1* (Supplementary Fig. S4), even though they include several AACXG motifs. Taken together, these results suggest that OsMYB102 indirectly represses the expression of *OsSGR* and *OsNYC1* through the OsABF4 regulatory network.

Overexpression of OsMYB102 affects growth and agronomic traits

In addition to its role in leaf senescence, ABA and its signaling components affect the growth and development of plants (Finkelstein, 2013). To examine the effect of *OsMYB102* overexpression on plant growth and development, we examined

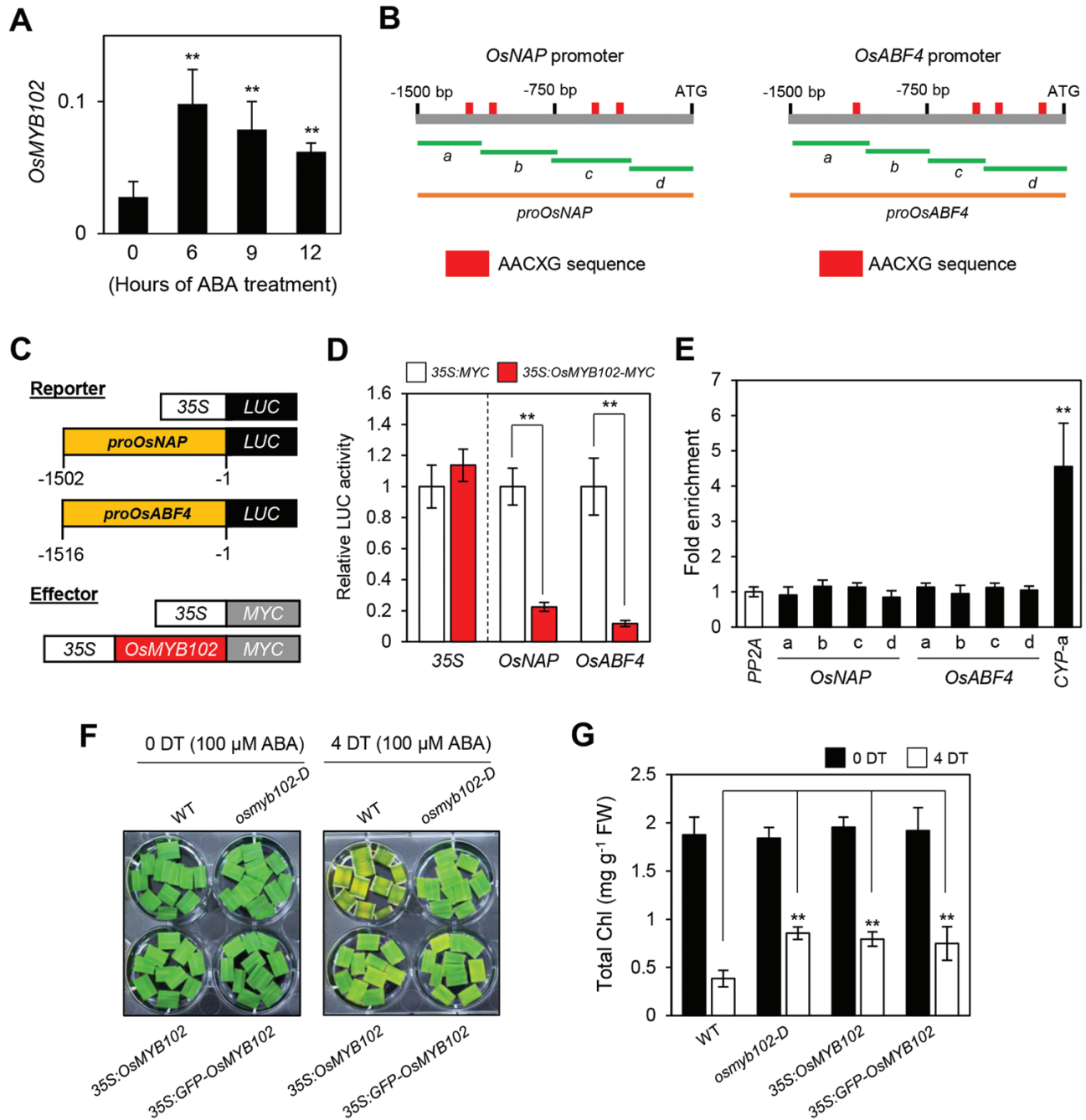


Fig. 7. OsMYB102 is involved in down-regulation of *OsNAP* and *OsABF4*. (A) The change in the expression level of *OsMYB102* during the treatment with 100 μM ABA. The transcript levels of *OsMYB102* were determined by RT-qPCR and normalized to the transcript levels of *UBQ5*. The mean and SD values were obtained from more than three biological samples. (B) The positions of the AACXG binding motif in the promoters of *OsNAP* and *OsABF4*, and the promoter fragments used for the ChIP assay (green horizontal lines) and the transactivation assay (orange horizontal lines). (C) Reporter and effector constructs used in the transrepression assay. Each construct also contained the NOS terminator (not shown). (D) The repression of the promoters of *OsNAP* (−1502 to −1) and *OsABF4* (−1516 to −1) by OsMYB102-MYC in the protoplast transient assay. The 35S promoter was used as a negative control. The mean and SD values were obtained from more than four biological samples. (E) OsMYB102 binding affinity to the promoter region of *OsNAP* and *OsABF4* in *planta* examined by ChIP assays. OsMYB102-MYC was transiently expressed in protoplasts isolated from 10-day-old WT seedlings. Fold-enrichment of the promoter fragments was measured by immunoprecipitation with an anti-MYC antibody (see Methods). *PP2A* was used as a negative control. (F, G) The changes of leaf color and total Chl content in WT, *osmyb102-D*, 35S:*OsMYB102*, and 35S:*GFP-OsMYB102* detached leaf discs during the treatment with 3 mM MES buffer (pH 5.8) containing 100 μM ABA. (A, D, E, G) Asterisks indicate a significant difference compared with the WT or negative control (Student's *t*-test, **P*<0.05, ***P*<0.01). The mean and SD values were obtained from more than five biological samples.

several agronomic traits in *osmyb102-D* plants at 180 d after sowing (DAS). The height of *osmyb102-D* plants was shorter than that of the WT (Fig. 9A). This phenotype was observed throughout development, including the early seedling

stage (Supplementary Fig. S5). Panicles were also shorter in *osmyb102-D* plants (Fig. 9C). Consistent with the short panicle length, *osmyb102-D* plants produced fewer grains per panicle and fewer branches per panicle than the WT (Fig. 9D, I). In

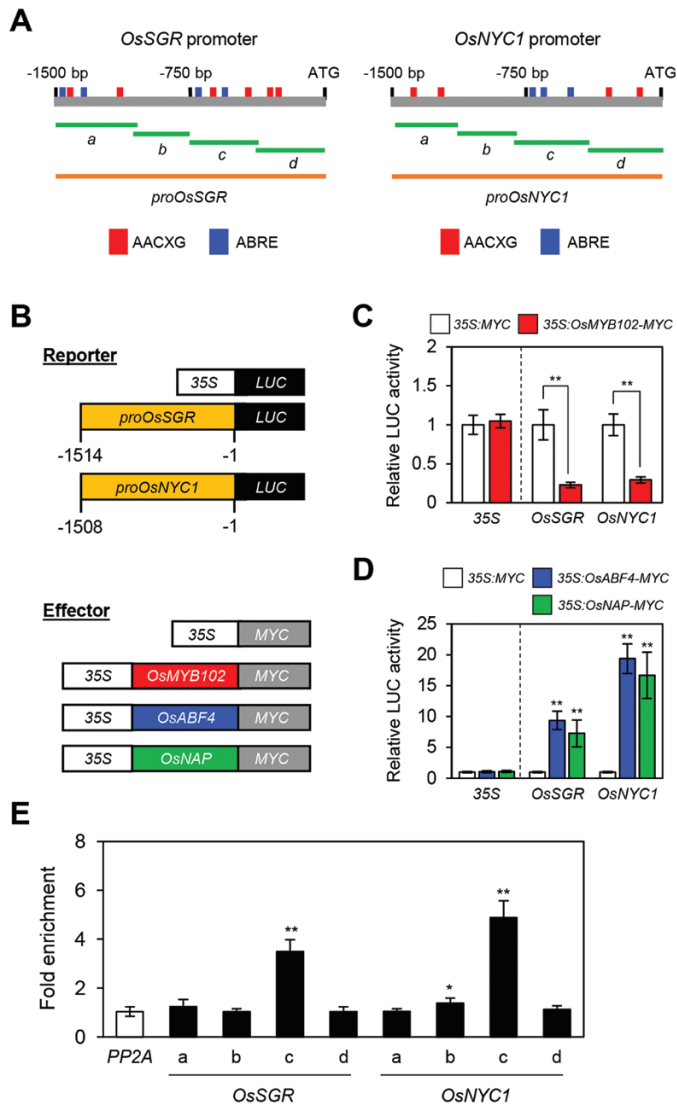


Fig. 8. OsABF4 directly activates the transcription of *OsSGR* and *OsNYC1*. (A) The positions of the AACXG and ABRE binding sequences in the promoters of *OsSGR* and *OsNYC1*, and the promoter fragments used for the ChIP assay (green horizontal lines) and the transactivation assay (orange horizontal lines). (B) Reporter and effector constructs used in the transrepression and transactivation assays shown in (C) and (D). Each construct also contained the NOS terminator (not shown). (C) The repression of the promoters of *OsSGR* (-1514 to -1) and *OsNYC1* (-1508 to -1) by *OsMYB102*-MYC in the protoplast transient assay. (D) The activation of the promoters of *OsSGR* and *OsNYC1* by *OsABF4*-MYC and *OsNAP*-MYC in the protoplast transient assay. (C, D) The 35S promoter was used as a negative control. (E) *OsABF4* binding affinity to the promoter regions of *OsSGR* and *OsNYC1* *in planta* examined by ChIP assays. *OsABF4*-MYC was transiently expressed in protoplasts isolated from 10-day-old WT seedlings. Fold-enrichment of the promoter fragments was measured by immunoprecipitation with an anti-MYC antibody (see Methods). *PP2A* was used as a negative control. (C, D, E) The mean and SD values were obtained from more than three biological samples. Asterisks indicate a significant difference compared with the negative control (Student's *t*-test, * $P < 0.05$, ** $P < 0.01$).

addition, spikelet fertility (Fig. 9E) was lower in *osmyb102-D* plants compared with the WT, leading to a decrease in grain weight (Fig. 9F) and grain yield per plant (Fig. 9G, H), and indicating that overexpression of *OsMYB102* negatively affects plant growth and agronomic traits.

Discussion

OsMYB102 negatively regulates leaf senescence by inhibiting ABA accumulation and the ABA signaling response

The role of ABA in the promotion of leaf yellowing has been widely studied. In Arabidopsis, the knockout mutants of *PYLACTIN RESISTANCE1-LIKE9* (*PYL9*) encoding an ABA receptor, *AAO3* encoding an ABA synthesis enzyme, *SUCROSE NONFERMENTING 1-RELATED PROTEIN KINASEs* (*SnRKs*), and genes encoding transcription factors related to the ABA signaling response, including *ABA-RESPONSIVE ELEMENT-BINDING FACTORS* (*ABFs*) including *ABF4* and *ABA INSENSITIVE 5* (*ABI5*), showed a stay-green phenotype during ABA- or dark-induced leaf senescence (Sakuraba *et al.*, 2014; Yang *et al.*, 2014; Gao *et al.*, 2016; Zhao *et al.*, 2016a). Moreover, Arabidopsis protoplasts transiently expressing *PYL9*, *SnRKs*, *ABFs*, and *ABI5* could activate the transcription of *SENESCENCE-ASSOCIATED GENE12* (*SAG12*) in a transactivation assay (Zhao *et al.*, 2016b), indicating the critical positive role of ABA in accelerating leaf senescence.

In this study, we identified a new transcription factor associated with ABA-induced leaf senescence in rice, *OsMYB102*. *OsMYB102* inhibits ABA accumulation by directly activating the transcription of *OsCYP707A6* (Fig. 6). *OsCYP707A6* is a functional homolog of Arabidopsis *CYP707A3*, which catalyses the key reaction of ABA degradation. Moreover, the Arabidopsis *cyp707a3* knockout mutant contained higher levels of ABA compared with WT (Umezawa *et al.*, 2006), strongly suggesting that *OsCYP707A6* has a crucial role in decreasing ABA accumulation. Although our results showed that *OsMYB102* directly activates *OsCYP707A6* transcription, the expression of *OsCYP707A6* decreased during leaf senescence (Supplementary Fig. S3), whereas *OsMYB102* transcription increased (Fig. 1A, B). We speculated that the expression of *OsCYP707A6* is mainly controlled by other unknown factor(s) and that *OsMYB102* acts as a regulator for avoiding a rapid decrease of *OsCYP707A6* transcript levels and preventing rapid accumulation of ABA in senescing leaves in rice. In addition, *OsMYB102* inhibits the ABA signaling response by down-regulating the expression of ABA-responsive genes, such as *OsNAP* and *OsABF4* (Fig. 7). Since the inhibition of ABA accumulation also leads to the down-regulation of the ABA-responsive genes *OsNAP* and *OsABF4*, it is probable that *OsMYB102* strongly represses the ABA signaling response at the transcriptional level (Fig. 10).

OsNAP is a homolog of Arabidopsis *NAP*, the first senescence-associated protein identified in Arabidopsis (Guo and Gan, 2006). *OsNAP* directly activates a few genes encoding CCEs, such as *OsSGR*, *OsNYC1*, and *OsPPH* (Liang *et al.*, 2014). Our ChIP assays showed that *OsABF4* directly interacts with the ABRE motif in the promoters of *OsSGR* and *OsNYC1* to up-regulate their transcript levels (Fig. 8). Similarly, Arabidopsis *ABF4* directly activates *AtNYC1* transcription to promote dark-induced senescence (Gao *et al.*, 2016); therefore, *ABF4* homologs have an important role in promoting leaf senescence in the dicot and monocot model plants Arabidopsis and rice, respectively,

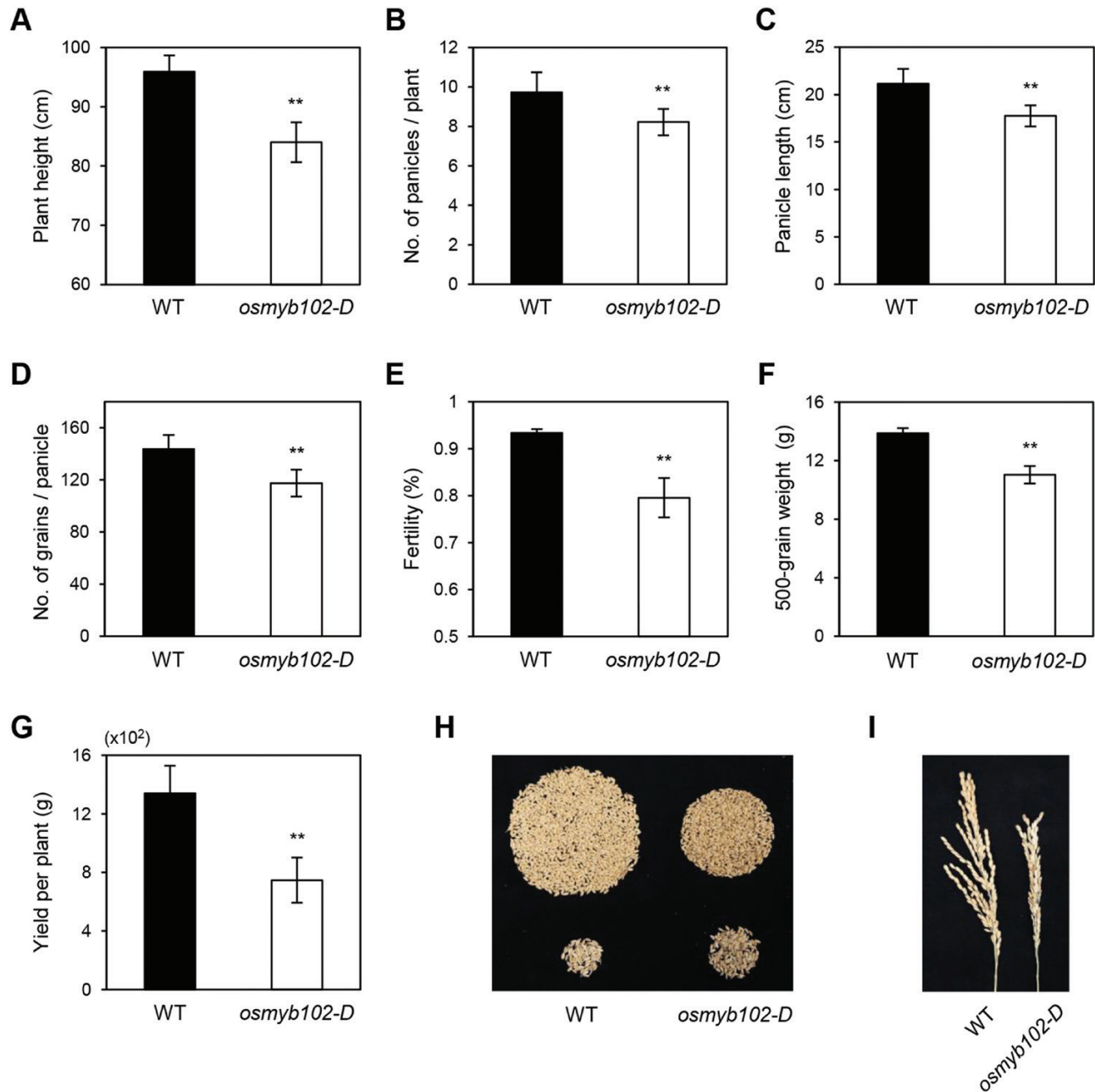


Fig. 9. Agronomic traits of *osmyb102-D* plants. Plant height (A), number of panicles per plant (B), panicle length (C), number of grains per panicle (D), fertility (E), 500-grain weight (F), grain yield per plant (G), images of the grains (top, fertile; bottom, sterile) (H), and panicle phenotype of main culm (I) were obtained from plants grown in the paddy field under natural LD conditions in 2017. The mean and SD values were obtained from at least 10 plant replicates. Asterisks indicate a significant difference between the WT and *osmyb102-D* plants (Student's *t*-test, * $P < 0.05$, ** $P < 0.01$).

by directly activating the expression of some CCE genes. In addition to ABF4, several TFs related to the ABA signaling response, such as ABF2, ABF3, ABI3, and ABI5, directly activate the expression of CCE genes (Delmas *et al.*, 2013; Sakuraba *et al.*, 2014; Gao *et al.*, 2016), indicating the crucial role of ABA signaling in the activation of CCE genes.

We found that in addition to altered expression of genes associated with ABA signaling and catabolism, the *osmyb102-D* plants also showed strong down-regulation of several SAGs, including rice *ETHYLENE INSENSITIVE3* (*OsEIN3*) and *OsMYC2* (Fig. 4). EIN3 acts as a central regulator of ethylene signaling, which promotes ethylene-induced leaf senescence

and DIS in Arabidopsis (Li *et al.*, 2013). A key TF in the JA response, MYC2 promotes methyl jasmonate-induced leaf senescence in Arabidopsis and rice (Qi *et al.*, 2015; Uji *et al.*, 2017). Therefore, it is probable that the delayed senescence phenotype of *osmyb102-D* plants is not only caused by modulation of ABA metabolism and signaling but also by inhibition of ethylene and JA signaling.

ABA is also involved in the regulation of many aspects of growth and development in plants (Finkelstein, 2013). ABA often acts as a growth promoter, since a number of ABA-deficient and ABA-insensitive mutants showed a stunted phenotype. Arabidopsis mutants of *ABA1*, encoding an ABA

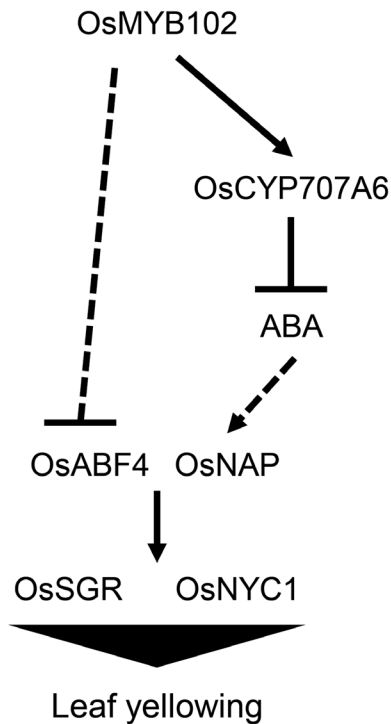


Fig. 10. Proposed model of the OsMYB102-mediated regulatory network of leaf senescence. OsMYB102 inhibits ABA biosynthesis by directly activating *OsCYP707A6*, which encodes an ABA catabolic enzyme. OsMYB102 indirectly represses the transcription of *OsNAP* and *OsABF4*, probably partially through the regulation of ABA biosynthesis. Then, *OsNAP* and *OsABF4* directly activate genes encoding Chl catabolic enzymes, such as *OsSGR* and *OsNYC1*, leading to leaf yellowing.

biosynthesis enzyme, show a severe stunted phenotype, which can be recovered by supplementing with ABA (Barrero *et al.*, 2005). In rice, an ABA-hyposensitive mutant, *spl3*, encoding a Mitogen-Activated Protein Kinase Kinase Kinase, is shorter in height and undergoes strongly delayed leaf senescence (Wang *et al.*, 2015). Similar to these ABA-deficient and ABA-insensitive mutants, the *osmyb102-D* and *OsMYB102-OX* lines had shorter plant heights throughout development compared with the WT (Fig. 9A; Supplementary Fig. S5). The *osmyb102-D* plants also had lower seed fertility (Fig. 9E), which is a typical phenotype of ABA-deficient and ABA-insensitive mutants. Collectively, our results show that OsMYB102 is involved in the regulation of various biological processes related to ABA.

OsMYB102 may be a functional homolog of AtMYB44, a multifaceted TF in Arabidopsis

Genome-wide classification of MYB TFs in Arabidopsis and rice has shown that OsMYB102 is a homolog of AtMYB44 (Katiyar *et al.*, 2012). Our ChIP assay showed that OsMYB102 binds to the promoter fragment that contains the AtMYB44 binding motif, AACXG (Fig. 6D). Furthermore, mutation analysis showed that the mutated promoter of *OsCYP707A6*, in which the AACAG sequence (−1139 to −1135 bp) was substituted to gggAG, was not strongly activated by co-transfection with OsMYB102 (Fig. 6F, G), indicating that OsMYB102 and AtMYB44 are functionally similar and commonly bind to

the AACXG sequence. *AtMYB44* is up-regulated in response to ABA treatment as well as several abiotic stresses, such as drought and high salinity (Jung *et al.*, 2008). In addition, *AtMYB44-OX* plants display a stay-green phenotype, similar to *osmyb102-D* plants, and knockout mutants of *AtMYB44* exhibit an early leaf yellowing phenotype (Jaradat *et al.*, 2013). This indicates that AtMYB44 also acts as a negative regulator of leaf senescence, probably by modulating ABA signaling and/or ABA accumulation. AtMYB44 interacts with the ABA receptors PYR1-LIKE8 (PYL8) and PYL9, decreasing their activities (Jaradat *et al.*, 2013; Li *et al.*, 2014). Therefore, it is probable that OsMYB102 can interact with the rice homologs of PYL8 and PYL9 to regulate ABA signaling. In ABA signaling or metabolism, the direct target genes of AtMYB44 have not been identified yet. Furthermore, it remains unclear whether the ABA concentration in leaves is altered by the knockout mutation or overexpression of *AtMYB44*. Therefore, the identification of conserved functions between AtMYB44 and OsMYB102 in ABA signaling and accumulation is necessary for understanding the significance of MYB44 homologs in leaf senescence.

AtMYB44 also has an important role in the drought stress response as a component of ABA signaling: *AtMYB44-OX* plants are hypersensitive to drought stress, while *atmyb44-KO* mutants are tolerant to drought stress (Jaradat *et al.*, 2013). However, we observed that both *osmyb102-D* and *OsMYB102-OX* plants were neither tolerant nor hypersensitive to dehydration stress (data not shown), suggesting that OsMYB102 is a functional homolog of AtMYB44 in leaf senescence, but their contributions to abiotic stress responses differ. AtMYB44 is also involved in defense to biotic stresses by modulating the signaling of ethylene, JA, and SA (Liu *et al.*, 2011; Shim *et al.*, 2013). Furthermore, a recent study revealed that AtMYB44 promotes the elongation of primary roots induced by *N*-3-oxo-hexanoyl-homoserine lactone (Zhao *et al.*, 2016a). Thus, AtMYB44 is a multifaceted TF that acts in many biological processes. To date, it is not clear whether OsMYB102 is also involved in defense to biotic stress by regulating the genes associated with ethylene, JA, and SA signaling. *ETHYLENE INSENSITIVE2 (EIN2)* was not induced in *osmyb102-D* (Fig. 4D), whereas it was strongly down-regulated in the *atmyb44* knockout mutant (Liu *et al.*, 2011), indicating that the contribution of OsMYB102 to biotic stress tolerance, if any, differs from that of AtMYB44. It will be interesting to examine whether OsMYB102 also functions in other biological processes.

Supplementary data

Supplementary data are available at *JXB* online.

Fig. S1. The *osmyb102* knockout mutant senescences faster than the wild-type during both dark- and ABA-induced senescence.

Fig. S2. Phytohormone biosynthesis and signaling genes were differentially expressed in *osmyb102-D* leaf discs during DIS.

Fig. S3. *OsCYP707A6* transcript levels decreased during natural and dark-induced leaf senescence.

Fig. S4. OsMYB102 does not bind to the promoter of *OsSGR* or *OsNYC1*.

Fig. S5. Overexpression of OsMYB102 decreases plant height.

Table S1. Primers used in this study.

Data deposition

Sequence data from this article can be found in the National Center for Biotechnology Information (NCBI) database under the following accession numbers: *OsNYC1*, Os01g0227100; *OsSGR*, Os09g0532000; *UBQ5*, Os01g0328400; *OsMYB102*, Os06g0637500; *OsNAP*, Os03g0327800; *OsABF4*, Os09g0456200; *OsCYP707A6*, Os08g0472800.

Acknowledgements

We thank Heeseong Kang for technical support for the generation of transgenic rice plants in this study, and Prof. Li-Jia Qu (Peking University, China) for providing the vectors for the CRISPR/Cas9 system in rice. This work was carried out with the support of the Cooperative Research Program for Agriculture Science & Technology Development (PJ013130), Rural Development Administration, South Korea, and Basic Science Research Program through the National Research Foundation (NRF) of Korea funded by the Ministry of Education (NRF-2017R1A2B3003310). The authors declare that they have no conflicts of interest.

References

- Balazadeh S, Riaño-Pachón DM, Mueller-Roeber B. 2008. Transcription factors regulating leaf senescence in *Arabidopsis thaliana*. *Plant Biology* **10**(Suppl 1), 63–75.
- Baldoni E, Genga A, Cominelli E. 2015. Plant MYB transcription factors: their role in drought response mechanisms. *International Journal of Molecular Sciences* **16**, 15811–15851.
- Barrero JM, Piqueras P, González-Guzmán M, Serrano R, Rodríguez PL, Ponce MR, Micol JL. 2005. A mutational analysis of the *ABA1* gene of *Arabidopsis thaliana* highlights the involvement of ABA in vegetative development. *Journal of Experimental Botany* **56**, 2071–2083.
- Besseau S, Li J, Palva ET. 2012. WRKY54 and WRKY70 co-operate as negative regulators of leaf senescence in *Arabidopsis thaliana*. *Journal of Experimental Botany* **63**, 2667–2679.
- Bohnert HJ, Nelson DE, Jensen RG. 1995. Adaptations to environmental stresses. *The Plant Cell* **7**, 1099–1111.
- Chen Y, Yang X, He K, *et al.* 2006. The MYB transcription factor superfamily of Arabidopsis: expression analysis and phylogenetic comparison with the rice MYB family. *Plant Molecular Biology* **60**, 107–124.
- Choi H, Hong J, Ha J, Kang J, Kim SY. 2000. ABFs, a family of ABA-responsive element binding factors. *The Journal of Biological Chemistry* **275**, 1723–1730.
- Cominelli E, Tonelli C. 2009. A new role for plant R2R3-MYB transcription factors in cell cycle regulation. *Cell Research* **19**, 1231–1232.
- Curtis MD, Grossniklaus U. 2003. A gateway cloning vector set for high-throughput functional analysis of genes in planta. *Plant Physiology* **133**, 462–469.
- Delmas F, Sankaranarayanan S, Deb S, Widdup E, Bournonville C, Bollier N, Northey JG, McCourt P, Samuel MA. 2013. ABI3 controls embryo degreening through Mendel's I locus. *Proceedings of the National Academy of Sciences, USA* **110**, E3888–E3894.
- Du H, Zhang L, Liu L, Tang XF, Yang WJ, Wu YM, Huang YB, Tang YX. 2009. Biochemical and molecular characterization of plant MYB transcription factor family. *Biochemistry (Moscow)* **74**, 1–11.
- Earley KW, Haag JR, Pontes O, Opper K, Juehne T, Song K, Pikaard CS. 2006. Gateway-compatible vectors for plant functional genomics and proteomics. *The Plant Journal* **45**, 616–629.
- Finkelstein R. 2013. Abscisic acid synthesis and response. *The Arabidopsis Book* **11**, e0166.
- Gao S, Gao J, Zhu X, Song Y, Li Z, Ren G, Zhou X, Kuai B. 2016. ABF2, ABF3, and ABF4 promote ABA-mediated chlorophyll degradation and leaf senescence by transcriptional activation of chlorophyll catabolic genes and senescence-associated genes in *Arabidopsis*. *Molecular Plant* **9**, 1272–1285.
- Guo Y, Gan S. 2006. AtNAP, a NAC family transcription factor, has an important role in leaf senescence. *The Plant Journal* **46**, 601–612.
- Hörtensteiner S. 2009. Stay-green regulates chlorophyll and chlorophyll-binding protein degradation during senescence. *Trends in Plant Science* **14**, 155–162.
- Hou K, Wu W, Gan SS. 2013. SAUR36, a small auxin up RNA gene, is involved in the promotion of leaf senescence in Arabidopsis. *Plant Physiology* **161**, 1002–1009.
- Huang CK, Lo PC, Huang LF, Wu SJ, Yeh CH, Lu CA. 2015. A single-repeat MYB transcription repressor, MYBH, participates in regulation of leaf senescence in Arabidopsis. *Plant Molecular Biology* **88**, 269–286.
- Jaradat MR, Feurtado JA, Huang D, Lu Y, Cutler AJ. 2013. Multiple roles of the transcription factor AtMYB1/AtMYB44 in ABA signaling, stress responses, and leaf senescence. *BMC Plant Biology* **13**, 192.
- Jung C, Kim YK, Oh NI, Shim JS, Seo JS, Choi YD, Nahm BH, Cheong JJ. 2012. Quadruple 9-mer-based protein binding microarray analysis confirms AACnG as the consensus nucleotide sequence sufficient for the specific binding of AtMYB44. *Molecules and Cells* **34**, 531–537.
- Jung C, Seo JS, Han SW, Koo YJ, Kim CH, Song SI, Nahm BH, Choi YD, Cheong JJ. 2008. Overexpression of AtMYB44 enhances stomatal closure to confer abiotic stress tolerance in transgenic Arabidopsis. *Plant Physiology* **146**, 623–635.
- Katiyar A, Smita S, Lenka SK, Rajwanshi R, Chinnusamy V, Bansal KC. 2012. Genome-wide classification and expression analysis of MYB transcription factor families in rice and Arabidopsis. *BMC Genomics* **13**, 544.
- Kim JH, Woo HR, Kim J, Lim PO, Lee IC, Choi SH, Hwang D, Nam HG. 2009. Trifurcate feed-forward regulation of age-dependent cell death involving miR164 in *Arabidopsis*. *Science* **323**, 1053–1057.
- Kim YS, Sakuraba Y, Han SH, Yoo SC, Paek NC. 2013. Mutation of the Arabidopsis NAC016 transcription factor delays leaf senescence. *Plant & Cell Physiology* **54**, 1660–1672.
- Kusaba M, Ito H, Morita R, *et al.* 2007. Rice NON-YELLOW COLORING1 is involved in light-harvesting complex II and grana degradation during leaf senescence. *The Plant Cell* **19**, 1362–1375.
- Kusaba M, Tanaka A, Tanaka R. 2013. Stay-green plants: what do they tell us about the molecular mechanism of leaf senescence. *Photosynthesis Research* **117**, 221–234.
- Lee SH, Sakuraba Y, Lee T, Kim KW, An G, Lee HY, Paek NC. 2015. Mutation of *Oryza sativa* CORONATINE INSENSITIVE 1b (OsCOI1b) delays leaf senescence. *Journal of Integrative Plant Biology* **57**, 562–576.
- Lee SM, Kang K, Chung H, Yoo SH, Xu XM, Lee SB, Cheong JJ, Daniell H, Kim M. 2006. Plastid transformation in the monocotyledonous cereal crop, rice (*Oryza sativa*) and transmission of transgenes to their progeny. *Molecules and Cells* **21**, 401–410.
- Li D, Li Y, Zhang L, *et al.* 2014. *Arabidopsis* ABA receptor RCAR1/PYL9 interacts with an R2R3-type MYB transcription factor, AtMYB44. *International Journal of Molecular Sciences* **15**, 8473–8490.
- Li Z, Peng J, Wen X, Guo H. 2013. *Ethylene-insensitive3* is a senescence-associated gene that accelerates age-dependent leaf senescence by directly repressing miR164 transcription in *Arabidopsis*. *The Plant Cell* **25**, 3311–3328.
- Liang C, Wang Y, Zhu Y, Tang J, Hu B, Liu L, Ou S, Wu H, Sun X, Chu J, Chu C. 2014. OsNAP connects abscisic acid and leaf senescence by fine-tuning abscisic acid biosynthesis and directly targeting senescence-associated genes in rice. *Proceedings of the National Academy of Sciences, USA* **111**, 10013–10018.
- Lim PO, Kim HJ, Nam HG. 2007. Leaf senescence. *Annual Review of Plant Biology* **58**, 115–136.
- Liu J, Osbourn A, Ma P. 2015. MYB transcription factors as regulators of phenylpropanoid metabolism in plants. *Molecular Plant* **8**, 689–708.
- Liu R, Chen L, Jia Z, Lü B, Shi H, Shao W, Dong H. 2011. Transcription factor AtMYB44 regulates induced expression of the *ETHYLENE*

- INSENSITIVE2* gene in *Arabidopsis* responding to a harpin protein. *Molecular Plant-Microbe Interactions* **24**, 377–389.
- Livak KJ, Schmittgen TD.** 2001. Analysis of relative gene expression data using real-time quantitative PCR and the $2^{-\Delta\Delta C_T}$ method. *Methods* **25**, 402–408.
- Mao C, Lu S, Lv B, Zhang B, Shen J, He J, Luo L, Xi D, Chen X, Ming F.** 2017. A rice NAC transcription factor promotes leaf senescence via ABA biosynthesis. *Plant Physiology* **174**, 1747–1763.
- Miao J, Guo D, Zhang J, Huang Q, Qin G, Zhang X, Wan J, Gu H, Qu LJ.** 2013. Targeted mutagenesis in rice using CRISPR-Cas system. *Cell Research* **23**, 1233–1236.
- Miao Y, Laun T, Zimmermann P, Zentgraf U.** 2004. Targets of the WRKY53 transcription factor and its role during leaf senescence in *Arabidopsis*. *Plant Molecular Biology* **55**, 853–867.
- Moore B, Zhou L, Rolland F, Hall Q, Cheng WH, Liu YX, Hwang I, Jones T, Sheen J.** 2003. Role of the *Arabidopsis* glucose sensor HXK1 in nutrient, light, and hormonal signaling. *Science* **300**, 332–336.
- Moschen S, Bengoa Luoni S, Di Rienzo JA, et al.** 2016. Integrating transcriptomic and metabolomic analysis to understand natural leaf senescence in sunflower. *Plant Biotechnology Journal* **14**, 719–734.
- Naito Y, Hino K, Bono H, Ui-Tei K.** 2015. CRISPRdirect: software for designing CRISPR/Cas guide RNA with reduced off-target sites. *Bioinformatics* **31**, 1120–1123.
- Oda-Yamamizo C, Mitsuda N, Sakamoto S, Ogawa D, Ohme-Takagi M, Ohmiya A.** 2016. Corrigendum: The NAC transcription factor ANAC046 is a positive regulator of chlorophyll degradation and senescence in *Arabidopsis* leaves. *Scientific Reports* **6**, 35125.
- Ooka H, Satoh K, Doi K, et al.** 2003. Comprehensive analysis of NAC family genes in *Oryza sativa* and *Arabidopsis thaliana*. *DNA Research* **10**, 239–247.
- Park SY, Yu JW, Park JS, et al.** 2007. The senescence-induced staygreen protein regulates chlorophyll degradation. *The Plant Cell* **19**, 1649–1664.
- Piao W, Kim EY, Han SH, Sakuraba Y, Paek NC.** 2015. Rice phytochrome B (OsPhyB) negatively regulates dark- and starvation-induced leaf senescence. *Plants* **4**, 644–663.
- Porra RJ, Thompson WA, Kriedemann PE.** 1989. Determination of accurate extinction coefficients and simultaneous equations for assaying chlorophylls *a* and *b* extracted with four different solvents: verification of the concentration of chlorophyll standards by atomic absorption spectroscopy. *Biochimica et Biophysica Acta* **975**, 384–394.
- Ptashne M, Gann AA.** 1990. Activators and targets. *Nature* **346**, 329–331.
- Qi T, Wang J, Huang H, Liu B, Gao H, Liu Y, Song S, Xie D.** 2015. Regulation of jasmonate-induced leaf senescence by antagonism between bHLH subgroup IIIc and IIId factors in *Arabidopsis*. *The Plant Cell* **27**, 1634–1649.
- Quirino BF, Normanly J, Amasino RM.** 1999. Diverse range of gene activity during *Arabidopsis thaliana* leaf senescence includes pathogen-independent induction of defense-related genes. *Plant Molecular Biology* **40**, 267–278.
- Sakuraba Y, Balazadeh S, Tanaka R, Mueller-Roeber B, Tanaka A.** 2012. Overproduction of chl B retards senescence through transcriptional reprogramming in *Arabidopsis*. *Plant & Cell Physiology* **53**, 505–517.
- Sakuraba Y, Han SH, Yang HJ, Piao W, Paek NC.** 2016. Mutation of *Rice Early Flowering3.1* (*OsELF3.1*) delays leaf senescence in rice. *Plant Molecular Biology* **92**, 223–234.
- Sakuraba Y, Jeong J, Kang MY, Kim J, Paek NC, Choi G.** 2014. Phytochrome-interacting transcription factors PIF4 and PIF5 induce leaf senescence in *Arabidopsis*. *Nature Communications* **5**, 4636.
- Sakuraba Y, Kim D, Paek NC.** 2018. Salt treatments and induction of senescence. *Methods in Molecular Biology* **1744**, 141–149.
- Sakuraba Y, Kim EY, Paek NC.** 2017. Roles of rice PHYTOCHROME-INTERACTING FACTOR-LIKE1 (*OsPIL1*) in leaf senescence. *Plant Signaling & Behavior* **12**, e1362522.
- Sakuraba Y, Piao W, Lim JH, Han SH, Kim YS, An G, Paek NC.** 2015. Rice ONAC106 inhibits leaf senescence and increases salt tolerance and tiller angle. *Plant & Cell Physiology* **56**, 2325–2339.
- Saleh A, Alvarez-Venegas R, Avramova Z.** 2008. An efficient chromatin immunoprecipitation (ChIP) protocol for studying histone modifications in *Arabidopsis* plants. *Nature Protocols* **3**, 1018–1025.
- Shim JS, Jung C, Lee S, Min K, Lee YW, Choi Y, Lee JS, Song JT, Kim JK, Choi YD.** 2013. AtMYB44 regulates WRKY70 expression and modulates antagonistic interaction between salicylic acid and jasmonic acid signaling. *The Plant Journal* **73**, 483–495.
- Takasaki H, Maruyama K, Takahashi F, Fujita M, Yoshida T, Nakashima K, Myouga F, Toyooka K, Yamaguchi-Shinozaki K, Shinozaki K.** 2015. SNAC-As, stress-responsive NAC transcription factors, mediate ABA-inducible leaf senescence. *The Plant Journal* **84**, 1114–1123.
- Uji Y, Akimitsu K, Gomi K.** 2017. Identification of OsMYC2-regulated senescence-associated genes in rice. *Planta* **245**, 1241–1246.
- Umezawa T, Okamoto M, Kushiro T, Nambara E, Oono Y, Seki M, Kobayashi M, Koshiba T, Kamiya Y, Shinozaki K.** 2006. CYP707A3, a major ABA 8'-hydroxylase involved in dehydration and rehydration response in *Arabidopsis thaliana*. *The Plant Journal* **46**, 171–182.
- Uno Y, Furihata T, Abe H, Yoshida R, Shinozaki K, Yamaguchi-Shinozaki K.** 2000. *Arabidopsis* basic leucine zipper transcription factors involved in an abscisic acid-dependent signal transduction pathway under drought and high-salinity conditions. *Proceedings of the National Academy of Sciences, USA* **97**, 11632–11637.
- Wang SH, Lim JH, Kim SS, Cho SH, Yoo SC, Koh HJ, Sakuraba Y, Paek NC.** 2015. Mutation of SPOTTED LEAF3 (*SPL3*) impairs abscisic acid-responsive signalling and delays leaf senescence in rice. *Journal of Experimental Botany* **66**, 7045–7059.
- Wu A, Allu AD, Garapati P, et al.** 2012. JUNGBRUNNEN1, a reactive oxygen species-responsive NAC transcription factor, regulates longevity in *Arabidopsis*. *The Plant Cell* **24**, 482–506.
- Yang J, Worley E, Udvardi M.** 2014. A NAP-AAO3 regulatory module promotes chlorophyll degradation via ABA biosynthesis in *Arabidopsis* leaves. *The Plant Cell* **26**, 4862–4874.
- Yang SD, Seo PJ, Yoon HK, Park CM.** 2011. The *Arabidopsis* NAC transcription factor VNI2 integrates abscisic acid signals into leaf senescence via the *COR/RD* genes. *The Plant Cell* **23**, 2155–2168.
- Yang SH, Choi D.** 2006. Characterization of genes encoding ABA 8'-hydroxylase in ethylene-induced stem growth of deepwater rice (*Oryza sativa* L.). *Biochemical and Biophysical Research Communications* **350**, 685–690.
- Yoo SD, Cho YH, Sheen J.** 2007. *Arabidopsis* mesophyll protoplasts: a versatile cell system for transient gene expression analysis. *Nature Protocols* **2**, 1565–1572.
- Zhang K, Halitschke R, Yin C, Liu CJ, Gan SS.** 2013. Salicylic acid 3-hydroxylase regulates *Arabidopsis* leaf longevity by mediating salicylic acid catabolism. *Proceedings of the National Academy of Sciences, USA* **110**, 14807–14812.
- Zhang Y, Su J, Duan S, et al.** 2011. A highly efficient rice green tissue protoplast system for transient gene expression and studying light/chloroplast-related processes. *Plant Methods* **7**, 30.
- Zhao Q, Li M, Jia Z, Liu F, Ma H, Huang Y, Song S.** 2016a. AtMYB44 positively regulates the enhanced elongation of primary roots induced by *N*-3-oxo-hexanoyl-homoserine lactone in *Arabidopsis thaliana*. *Molecular Plant-Microbe Interactions* **29**, 774–785.
- Zhao Y, Chan Z, Gao J, et al.** 2016b. ABA receptor PYL9 promotes drought resistance and leaf senescence. *Proceedings of the National Academy of Sciences, USA* **113**, 1949–1954.